Environmental Science and Pollution Research
https://doi.org/10.1007/s11356-024-32380-4

RESEARCH ARTICLE

Integrated approaches for heavy metal–contaminated soil remediation: harnessing the potential of *Paulownia elongata* S. Y. Hu, *Oscillatoria* sp., arbuscular mycorrhizal fungi (*Glomus mosseae* and *Glomus intraradices*), and iron nanoparticles

Sara Khoshyomn[1] · Ava Heidari[1] · Mohammad Farzam[2] · Zeinab Shariatmadari[3] · Zahra Karimian[4]

Received: 30 June 2023 / Accepted: 4 February 2024

Abstract

In recent years, researchers have extensively investigated the remediation of heavy metal–contaminated soil using plants, microorganisms, and iron nanoparticles. The objective of this study was to investigate and compare the individual and simultaneous effects of *Paulownia elongata* S. Y. Hu, cyanobacteria (*Oscillatoria* sp.), arbuscular mycorrhizal fungi (AMF) including *Glomus mosseae* and *Glomus intraradices*, and zero-valent iron nanoparticles (nZVI) on the remediation of heavy metal–contaminated soil containing chromium (Cr VI and Cr III) and nickel (Ni). The study found significant variations in parameters such as pH (acidity), electrical conductivity (EC), nitrogen (N), phosphorus (P), potassium (K), and organic carbon (OC) among different treatments. The addition of cyanobacteria, AMF, and nZVI influenced these properties, resulting in both increases and decreases compared to the control treatment. The treatment involving a combination of cyanobacteria, AMF, and nZVI (CCAN25) exhibited the highest increase in growth parameters, such as total dry mass, root length, stem diameter, and leaf area, while other treatments showed varied effects on plant growth. Moreover, the CCAN25 treatment demonstrated the highest increase in chlorophyll *a*, chlorophyll *b*, and carotenoid levels, whereas other treatments displayed reductions in these pigments compared to the control. Moderate phytoaccumulation of Cr and Ni in *P. elongata* samples across all treatments was observed, as indicated by the bioconcentration factor and bioaccumulation coefficient values being less than 1.0 for both metals. The findings provide insights into the potential application of these treatments for soil remediation and plant growth enhancement in contaminated environments.

Keywords Chromium · Nickel · Bioremediation · Phytoremediation · *Oscillatoria* sp

Introduction

Industrial growth has led to the widespread consumption of various chemicals, resulting in harmful residues that pose a threat to the environment. One significant consequence is the contamination of soil with heavy metals, a concern highlighted by Han et al. (2019). Heavy metals are hazardous pollutants that pose a serious threat to the food chain due to their toxicity, high stability, accumulation, and biomagnification. Not only do they devastate ecosystems, but they are also transmitted to humans through the consumption of aquatic animals or plants grown in contaminated habitats (Li et al. 2019).

Fortunately, diverse remediation techniques, including physical, chemical, and biological remediation techniques, are available for the cleanup of heavy metal–contaminated

Responsible Editor: Elena Maestri

✉ Ava Heidari
ava.heidari@yahoo.com

[1] Department of Environmental Science, Faculty of Natural Resources and Environment, Ferdowsi University of Mashhad, Mashhad, Iran

[2] Department of Range and Watershed Management, Faculty of Natural Resources and Environment, Ferdowsi University of Mashhad, Mashhad, Iran

[3] Faculty of Biosciences, Shahid Beheshti University, G.C. Evin, Tehran, Iran

[4] Department of Ornamental Plants, Research Center for Plant Sciences, Ferdowsi University of Mashhad, Mashhad, Iran

Published online: 16 February 2024

soil (Shah and Daverey 2020; Tian et al. 2019). Phytoremediation is a plant-mediated decontamination process that involves the use of shrubs and trees in conjunction with microorganisms (Cameselle et al. 2019; Gomes 2012). This method is often referred to as green technology, as it harnesses nature's ability to clean up pollution (Buzan et al. 2018; Shah and Daverey 2020). Phytoremediation is widely promoted as an effective, low-cost, easy-to-use, practical, economically viable, aesthetically pleasing, and widely accepted technology (Parmar and Singh 2015; Shah and Daverey 2020).

Plants play a crucial role in phytoremediation by absorbing essential heavy metals like Cu, Fe, and Ni for their growth and accumulating highly toxic heavy metals such as As, Hg, Pb, and Cr (Forte and Mutiti 2017; Han et al. 2017; Marrugo-Negrete et al. 2015). Notably, tree species from the genus *Paulownia*, particularly *P. elongata*, have shown success in phytoremediation due to their rapid growth, high biomass, tolerance to heavy metals, and minimal entry into the food chain (Azzarello et al. 2012; Buzan et al. 2018; Doumett et al. 2008, 2010; Zhang et al. 2010). *Paulownia*, a genus of *Paulownians* from the Lamiaceae family, is known for its digitalis-like flowers and large heart-shaped leaves. During the initial year of growth, the stem diameter of *Paulownia* can reach 2 cm. This species has an average fiber length of 1.11 mm, with an average cell cavity width of 24.47 µm and a wall thickness of 4.4 µm. Several studies have reported the successful phytoremediation of specific heavy metals using *P. elongata* species. *P. tomentosa* Steud. has been utilized for the remediation of Pb and Cd (Liu et al. 2007); *P. fortunei* Seem. for Mn (Zhang et al. 2020); *P. tomentosa* for Zn (Azzarello et al. 2012); *P. tomentosa* for Zn (Bahri et al. 2014); *P. tomentosa* for Cu, Pb, and Zn (Doumett et al. 2010); and *P. fortunei* for Pb, Zn, Cu, and Cd (Zhang et al. 2010).

The coexistence of different mycorrhizal fungi species in plants growing in heavy metal–contaminated soils has proven effective in protecting plant roots, promoting growth, and enhancing biomass accumulation (Ma et al. 2019). Mycorrhizal fungi, including *Glomus mosseae* and *Glomus intraradices*, offer a cost-efficient strategy for remediating contaminated soils (Mokarram-Kashtiban et al. 2019). Positive impacts on phytoremediation, such as the reduction of chemical toxicity caused by heavy metals, have been reported by Riaz et al. (2021) and Krishnamoorthy et al. (2019). Furthermore, Leung et al. (2013) demonstrated that mycorrhizal fungi enhance detoxification, nutrient absorption, and protection against metal toxicity, thereby improving plant efficiency in phytoremediation.

Introducing nanotechnology into phytoremediation, nano-phytoremediation combines nanotechnology and phytotechnology to address environmental pollution (Jesitha and Harikumar 2018). This approach utilizes engineered nanomaterials, particularly iron-based nanoparticles like nano-zero-valent iron (nZVI), for enhanced pollutant transformation and detoxification efficiency (Jesitha and Harikumar 2018; Ma et al. 2013). nZVI, with its non-toxic nature, cost-effectiveness, abundance, and large specific surface area, has gained recognition for soil remediation (Jiang et al. 2018; Li et al. 2021; Xu et al. 2012a, 2012b). Studies have demonstrated its efficacy in immobilizing heavy metals in soil, reducing their mobility and bioavailability (Zhang et al. (2010), Gil-Díaz et al. (2016), Mar Gil-Díaz et al. (2014), Dorjee et al. (2014), Su et al. (2016), Huang et al. (2018). Moreover, the presence of nZVI and microorganisms concurrently can influence the availability of heavy metals (Fajardo et al. 2012; Hansel et al. 2011). Furthermore, nZVI has a significant impact on soil microorganisms, nutrients, and contaminants (Liu et al. 2022).

This study endeavors to explore integrated approaches for the remediation of heavy metal–contaminated soil, focusing on the combined utilization of *P elongata* S. Y. Hu, *Oscillatoria* sp., arbuscular mycorrhizal fungi (*G. mosseae* and *G. intraradices*), and iron nanoparticles. By combining these separate but complementary techniques, we aim to harness their synergistic potential in addressing the specific heavy metals, namely, Cr(VI), Cr(III), and Ni, in the contaminated soil. While previous studies (Mokarram-Kashtiban et al. 2019; Sang et al. 2021) have investigated the individual use of components like nZVI and AMF, our research represents a pioneering effort in exploring the simultaneous and synergistic effects of these elements in the context of phytoremediation.

Materials and methods

Chemicals

Merck supplied sodium hexametaphosphate ($(NaPO_3)_6$), acetone (C_3H_6O), ethanol (C_2H_6O), hydrochloric acid (HCl), hydrogen peroxide (H_2O_2) 35%, diphenyl carbazide, nitric acid (HNO_3) 65% and ammonium acetate ($C_2H_4O_2{\cdot}H_3N$), and acetic acid ($C_2H_4O_2$). Sigma Aldrich provided magnesium carbonate ($MgCO_3$), hydroxylamine hydrochloride, and nickel nitrate ($Ni(NO_3)_2{\cdot}6H_2O$). Potassium dichromate ($K_2Cr_2O_7$) was purchased from Biopharm Inc. NZI was acquired from US Research Nanomaterials, Inc. All chemicals and reagents utilized in this study were of analytical grade.

Soil

The soil used in this study was collected from a location 15 km northeast of Mashhad, Iran, at a latitude of 36°22′25.8″ and a longitude of 59°32′2.02″. After air-drying,

the soil was passed through a 2-mm sieve. Its texture was determined to be sandy clay loam. Table 1 provides details of soil characteristics, including pH, EC, nitrogen, phosphorus, potassium contents, and organic carbon. The deliberate objective was to intentionally introduce Cr and Ni contamination to the soil, specifically to tackle the distinct challenges associated with these metals in Mashhad, Iran (Baratzadeh Poustchi et al. 2020; Mohammadpouran et al. 2009). Besides, Cr(VI) is a toxic heavy metal known to inhibit plant growth, with many plants unable to tolerate even low concentrations of this metal (Zulfiqar et al. 2023). In alignment with previous studies (Aydinalp and Marinova 2009; Saravanan et al. 2019; Ullah et al. 2019), a conservative concentration of 5 ppm was chosen for the phytoremediation experiment to ensure a tolerable environment for plant growth. Initially, the soil samples were free of Cr(VI) and contained 4 ppm Ni. To achieve the desired contamination levels of 5 ppm Cr(VI) and 25 ppm Ni, the soil was spiked. This was done by applying 5 mL of a stock solution of Cr(VI) (prepared by dissolving 2.835 g of $K_2Cr_2O_7$ in 1 L of deionized water) and 25 mL of a stock solution of Ni (prepared by dissolving 4.97 g of Ni $(NO_3)2{\cdot}6H_2O$ in 1 L of deionized water) per kilogram of soil.

Nano-zero-valent iron addition

Based on previous research conducted by Mokarram-Kashtiban et al. (2019), two doses of nZVI, namely, 25 mg/kg and 75 mg/kg, were selected to be applied to the soil. To prepare the nZVI solutions, different concentrations of nZVI (25 mg/kg and 75 mg/kg) were mixed with 50 mL of deionized water and shaken for 10 min. Subsequently, the resulting mixture was evenly distributed over the soil surface, with a total quantity of 1 kg, and thoroughly mixed. the mixture was then poured (1 kg) onto the soil surface and mixed.

Experimental pot preparation

The soil was placed in plastic pots with a diameter of 22 cm and a height of 25 cm. Before planting, the pots were irrigated with 75% of the field capacity. The plant species (*Paulownia elongata* S. Y. Hu, family: Paulowniaceae) were identified and authenticated by at Ferdowsi University of Mashhad Herbarium (FUMH), Mashhad, Iran. A voucher specimen (FUMH, no. 45510) has been deposited in the herbarium. Seedlings of *P. elongata*, with a height ranging from 80 to 90 cm, were obtained from the greenhouse at the Ferdowsi University of Mashhad, located in Mashhad. On February 4th, 2020, the seedlings were transplanted into pots containing 3 kg of soil. The pots were then placed in a greenhouse with a temperature range of 21 to 31 °C, providing 16 h of light and 8 h of darkness (with an intensity of 1600 lx). Daily irrigation of the pots was carried out using tap water at 75% of the field capacity. The experiments were conducted using a completely randomized design, with the following treatments. The experimental setup comprised four replicates for each treatment.

AMF inoculation

The AMF was provided by Turan Biotech Co. in Iran. A quantity of 10 g of AMF was placed in each pot. To facilitate its coexistence with the plant roots, the fungus was added to the soil in layers.

Cyanobacteria inoculation

Before inoculation, the soil was sterilized at 121 °C for 30 min. In a sterile Erlenmeyer flask, 0.8 g of purified cyanobacteria was stirred for 16 h.

Table 1 Treatments and their abbreviations

Treatment	Abbreviations
Non-contaminated soil	NC
Contaminated soil	C
Contaminated soil + AM	CA
Contaminated soil + cyanobacteria	CC
Contaminated soil + nano-sized zero-valent iron 25	CN25
Contaminated soil + nano-sized zero-valent iron 75	CN75
Contaminated soil + cyanobacteria + AM	CCA
Contaminated soil + cyanobacteria + nano-sized zero-valent iron 25	CCN25
Contaminated soil + cyanobacteria + nano-sized zero-valent iron 75	CCN75
Contaminated soil + cyanobacteria + AM + nano-sized zero-valent iron 25	CCAN25
Contaminated soil + cyanobacteria + AM + nano-sized zero-valent iron 75	CCAN75

Harvesting

After washing the plants with distilled water, the growth parameters such as stem length, root length, and leaf area were measured using a leaf area meter (Licow) calibrated to 0.001 cm^2. The leaf area was calculated using the Bioleaf software. The plants were classified based on their root, stem, and leaf characteristics. The mycorrhizal roots were collected and analyzed to determine the percentage of colonization. Furthermore, the roots, stems, and leaves were dried at 70 °C for 72 h before being weighed.

Mycorrhizal colonization

Root staining was performed according to the methodology outlined by Phillips and Hayman (1970) to assess the extent of root colonization in treatments containing AMF. Delicate, filamentous roots were excised and positioned in a Petri dish. A 10% KOH solution, approximately 10 drops, was applied to ensure adequate coverage, followed by exposure to a warm water bath at 90 °C for 1 h. After this treatment, roots were extracted and subjected to a triple wash with distilled water to eliminate residual discoloration.

Following the washing steps, a few drops of a 1% HCl solution were introduced to the roots. After 5 min, without additional rinsing (solely the removal of excess acid), approximately 1 to 2 drops of a Trypan blue solution were administered. Following an additional 10 min, a color-fixing solution (lactic acid) was introduced to the sample, removing any surplus coloration and adding 1 to 2 drops of color fixative. After a subsequent 5-min period, roots were carefully transferred from the Petri dish to a microscope slide for microscopic analysis. The discerned blue circles in the images correspond to fungal structures within the root tissues. Microscopic images were captured and processed using JMV (J Micro Vision) software to quantify the percentage of root colonization.

Soil analysis

The pH and EC values of the soil were determined following the method described by Mylavarapu et al. (2020). The pH was measured using a pH meter (model + 20; Crison, Spain) in a 1:25 soil-to-deionized water mixture, which was shaken for 1 h at 25 °C. Soil EC was measured using an EC meter (model 4510; Jenway, England) in a 1:25 soil-to-deionized water ratio. Organic carbon content was determined using the method outlined by Park et al. (2017), while nitrogen content was analyzed using the Kjeldahl method (Bremner 1960). Phosphorus content was determined using the Olsen method (Olsen 1954), and potassium content was analyzed according to the procedure described by Rowell (1994).

Measurement of heavy metal concentrations in soil

Measurement of heavy metal concentrations in soil was performed using the sequential extraction method (BCR), as reported by Wuana et al. (2010). This method consists of four consecutive stages. Initially, 1 g of soil was dried in an oven at 105 °C for 2 h. In the first stage, 1 g of soil was placed in an Erlenmeyer flask, and 11.0 mM lactic acid (40 mL) was added. The mixture was incubated at room temperature for 16 h. Subsequently, it was centrifuged at 1500 rpm for 15 min. The resulting supernatant was extracted and kept at 4 °C until spectrophotometric analysis. The remaining soil residue was centrifuged with approximately 20 mL of distilled water, following the previous method, and the resulting supernatant was discarded. In the second stage, the remaining soil residue from the previous step was treated with 5.0 mM hydrochloric acid hydroxylamine solution (40 mL), and the resulting supernatant was extracted and kept at 4 °C. In the third stage, the soil residue from stage 2 was treated with 8.8 mM hydrogen peroxide solution (10 mL) and shaken at room temperature for 1 h. The solution was then placed in a water bath at 85 °C for 1 h. After cooling, 1.0 M ammonium acetate (50 mL) was added to the solution, which was incubated at room temperature for 16 h. The resulting supernatant was kept at 4 °C, similar to the previous stages. In the final stage, the remaining soil residue was treated with 17.0 M nitric acid (12.5 mL) and 12.0 M hydrochloric acid (5.37 mL) and incubated at room temperature for 24 h. Then, the samples were subjected to at 130 °C for 15 min, passed through Whatman filter paper no. 42, and the clear liquid was kept at 4 °C. The absorbance of Cr(VI) capacity in the digestion solutions was measured at 540-nm wavelength using a UV–visible spectrophotometer (DR5000UV-Visible; Hach, USA) after adding 2.0 mL of diphencylcarbazide solution. For the measurement of total chromium and nickel, an ICP instrument (76004555 Spectro; Arcos, Germany) was used.

Plant analysis

Measurement of heavy metal concentrations in P. elongata

According to the method described by Ashrafi et al. (2015), the roots, stems, and leaves of the plant were initially dried in an oven at 70 °C for 24 h. Following this, 25 mL of nitric acid was added, and the mixture was heated at 110 °C for 2 h. Subsequently, 5 mL of hydrogen peroxide was added, and the mixture was boiled in a digestion unit for 1 h. After cooling, the solution was filtered through a Whatman No. 42 filter paper. Then, 0.2 mL of a diphenylcarbazide solution

(0.25 g of diphenylcarbazide in 50 mL of acetone) was added to the filtered solution. After 2 min, the absorption of Cr(VI) was measured at a wavelength of 540 nm using a UV–visible spectrophotometer, and its concentration was calculated. To determine the total concentration of chromium and nickel, the samples were analyzed using ICP (inductively coupled plasma) analysis. The concentration of Cr(III) was determined by subtracting the concentrations of total chromium and Cr(VI).

Photosynthetic pigments in soil and plants

To measure chlorophyll in soil, a mixture of 1 g of soil, 5 mL of 99.9% ethanol, and 0.05 g of magnesium carbonate was prepared and stored at 80 °C for 5 min. Subsequently, the solution was centrifuged at 3000 rpm for 10 min. The amount of chlorophyll in the solution was determined using a UV–visible spectrophotometer (DR5000; Hach) at wavelengths of 649, 665, and 750 nm. The concentration of chlorophyll *a*, chlorophyll *b*, and carotenoids were calculated using the following formulas:

$$\text{Chlorophyll } a\ [\text{mg}] = (19.3 * \text{A663} - 0.86 * \text{A645})\text{V}/100\ \text{W} \quad (1)$$

$$\text{Chlorophyll } b[\text{mg}] = (19.3 * \text{A645} - 3.6 * \text{A663})\text{V}/100\ \text{W} \quad (2)$$

$$\text{Carotenoid } s[\text{mg}] = 10\ (\text{A470}) - 3.27(\text{mgChl.}a) - 104(\text{mg Chl.}b)/227 \quad (3)$$

Results and discussion

Cyanobacteria and AMF

Figure 1 depicts images of cyanobacteria and AMF captured using a light microscope after incubation. Based on morphological analysis and comparison with Ahemad and Khan (2012), it can be concluded that the purified species bears a resemblance to *Oscillatoria* sp. This species lacks heterocysts, branching, exhibits slight curvature at the ends, and is straight, filamentous, and sometimes possesses a thin mucilaginous sheath. The morphological examination of cyanobacterial cells in the image reveals that the size and diameter of cyanobacterial cells range from 1 to 40 µm. The cell wall resembles the cell wall of gram-negative bacteria. Regarding AMF, through morphological examination and comparison with Wu et al. (2015), it has been established that the observed blue circles represent fungal structures known as vesicular mycorrhiza located inside the root.

Cyanobacteria on the soil surface

Figure 2 shows SEM images of cyanobacterial growth on the surface of contaminated soil under different treatments. As observed in the figures, the growth of cyanobacteria is more extensive in the CN75 treatment compared to when cyanobacteria were inoculated alone (CC treatment). It also appears that in the treatment with AMF (CCA), the growth of cyanobacteria on the contaminated soil surface is limited, whereas the growth of cyanobacteria on the soil surface in the CCAN25 and CCAN75 treatments is somewhat more extensive than in the CCA treatment. It is good to mention that, before treatment application, the experimental soils were subjected to sterilization, resulting in the elimination of all microorganisms, including filamentous fungi. As a consequence, the discernible hyphae observed in the SEM images depicted in Fig. 2 are attributable to the AMF.

Physical and chemical properties of soil

Table 2 provides information on the acidity, electrical conductivity (EC), nitrogen, phosphorus, potassium, and organic carbon levels of soil samples in various treatments as part of the study.

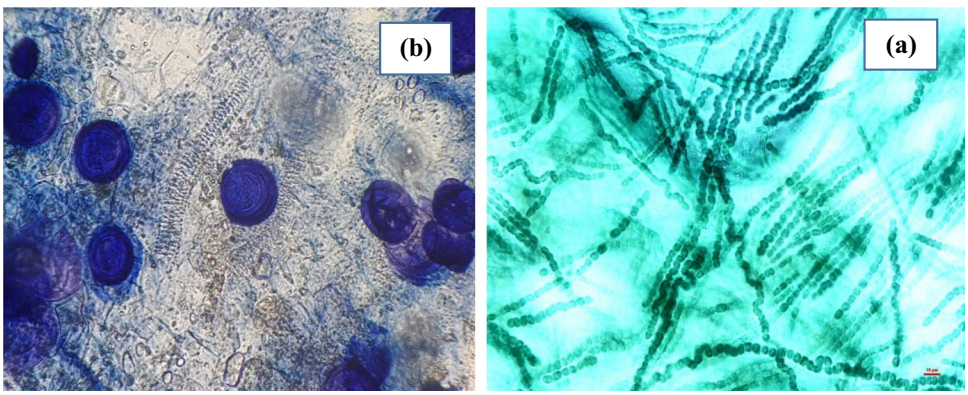

Fig. 1 The images of cyanobacteria (**a**) and AMF (**b**) inoculated to soil

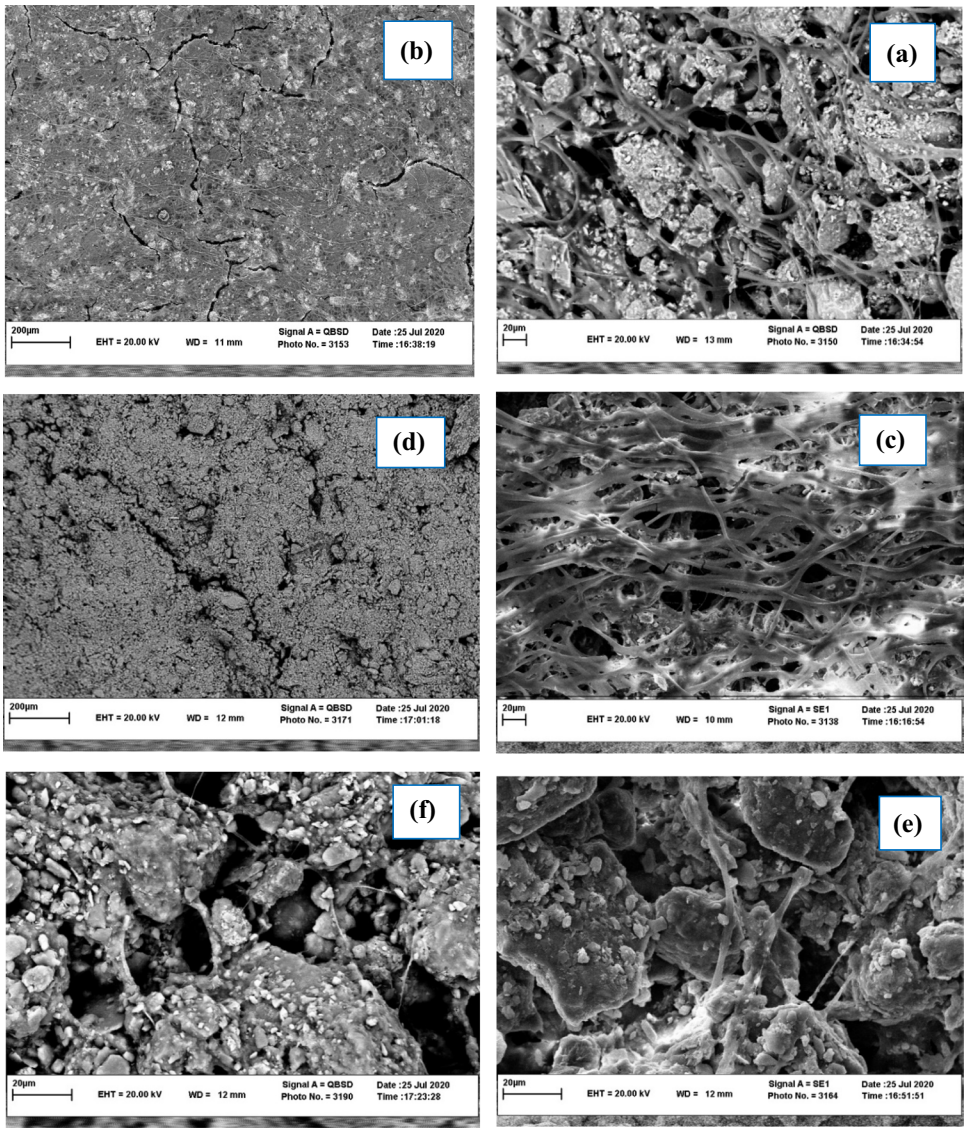

Fig. 2 SEM images of cyanobacterial growth on the surface of contaminated soil: **a** CC; **b** CN25; **c** CN75; **d** CCA; **e** CCAN25; **f** CCAN75

Table 2 Mean comparison of physical and chemical properties of soil

Treatment	pH	EC (dS/m)	N (mg/kg)	P (mg/kg)	K (mg/kg)	OC (mg/kg)
C	8.74 ± 0.02^{A}	668 ± 0.91^{C}	280 ± 0.005^{H}	60.39 ± 0.01^{B}	98.86 ± 0.04^{D}	6.65 ± 0.01^{C}
CA	8.61 ± 0.01^{A}	567 ± 0.09^{D}	252 ± 0.025^{I}	24.30 ± 0.02^{E}	93.17 ± 0.01^{E}	7.61 ± 0.01^{AB}
CC	8.48 ± 0.08^{A}	345 ± 1.12^{G}	351 ± 0.023^{D}	21.01 ± 0.02^{G}	79.21 ± 0.01^{G}	7.79 ± 0.05^{AB}
CN25	8.58 ± 0.04^{A}	798 ± 0.09^{B}	238 ± 0.014^{J}	21.97 ± 0.01^{F}	80.13 ± 0.01^{G}	6.15 ± 0.01^{D}
CN75	8.66 ± 0.02^{A}	875 ± 1.19^{A}	212 ± 0.012^{K}	44.25 ± 0.05^{D}	140.31 ± 0.01^{A}	6.24 ± 0.01^{D}
CCA	8.44 ± 0.03^{A}	479 ± 1.75^{E}	422 ± 0.012^{A}	22.64 ± 0.01^{F}	104.61 ± 0.01^{C}	7.75 ± 0.02^{AB}
CCN25	8.55 ± 0.07^{A}	612 ± 1.15^{CD}	345 ± 0.013^{E}	18.14 ± 0.03^{G}	85.68 ± 0.01^{F}	7.95 ± 0.01^{A}
CCN75	8.51 ± 0.04^{A}	589 ± 1.25^{D}	338 ± 0.001^{F}	66.73 ± 0.02^{A}	133.64 ± 0.02^{B}	6.08 ± 0.01^{D}
CCAN25	8.41 ± 0.06^{A}	347 ± 1.96^{FG}	411 ± 0.010^{B}	23.13 ± 0.01^{F}	92.23 ± 0.08^{E}	7.54 ± 0.01^{B}
CCAN75	8.49 ± 0.01^{A}	375 ± 0.85^{F}	379 ± 0.010^{C}	23.33 ± 0.01^{EF}	80.12 ± 0.01^{G}	7.68 ± 0.01^{AB}

Different letters indicate statistical significance

Electrical conductivity

The control sample (C) had an electrical conductivity of 668 µS/m. All treatments, except CCN25, showed significant differences from the control (Table 2). The highest EC values were associated with the CN75 (+31%) and CN25 (19%) treatments. However, the lowest EC was related to CC treatment (−48%) and other treatments with cyanobacteria. Inoculation of cyanobacteria in the soil, either alone or in combination with NZI and AM, reduces EC significantly.

Nutrients (nitrogen, phosphorus, potassium)

According to Table 2, the amount of N in the control treatment (C) was 280 mg/kg. A significant change was observed between all treatments compared to the control. The CCA (+50%) and CN75 (−25%) treatments showed the highest significant rise in nitrogen compared to the control. This suggests that using high amounts of iron nanoparticles (75 mg/kg) separately results in the highest substantial reduction in soil nitrogen content. The most significant increase in nitrogen content is produced when cyanobacteria and arbuscular mycorrhizal are applied together.

The phosphorus content of the control treatment (C) was 60.39 mg/kg. When compared to the control, all treatments showed a significant difference. The CCN75 treatment (+10%) exhibited the highest significant increase in phosphorus while the CCN25 (−70%) and CC (−65%) had the highest substantial decreases compared to the control. This indicates that the most substantial rise in phosphorus content is obtained when cyanobacteria are used simultaneously with a high amount of iron nanoparticles (75 mg/kg), and a significant decrease is acquired when the cyanobacteria are used with a low amount of iron nanoparticles (25 mg/kg).

The potassium concentration in the control treatment (C) was 98.86 mg/kg. A substantial difference was seen between all treatment and control samples. The CN75 treatment (+42%) had the highest significant increase in potassium while the CC (−19%), CCAN75 (−18%), and CN25 (−18%) treatments showed the maximum significant reductions, relative to the control sample. This suggests that when 75 mg/kg of iron nanoparticles are utilized separately, the most substantial increase in potassium content is produced. The most substantial reduction was related to using 25 mg/kg of iron nanoparticles simultaneously with AMF and cyanobacteria compared to the control.

Organic carbon

Soil organic carbon in the control sample was 6.65 mg/kg. A significant change was observed between all treatments compared to the control treatment. The CCN25 (+20%) treatment had the most significant increase in organic carbon. In addition, the CCN75 (−8.5%), CN25 (−7.5%), and CN75 (−6%) treatments showed the most substantial reductions in comparison to the control treatment. This suggests that the highest substantial rise was attained when cyanobacteria and 25 mg/kg of iron nanoparticles were used simultaneously. Besides, the presence of 75 mg/kg of iron nanoparticles in treatments reduced the amount of organic carbon significantly compared to the control.

Plant growth

Table 3 shows the influence of various treatments (e.g., nZVI, cyanobacteria, and AM) on *P. elongata* growth metrics and root colonization by the AM fungus in contaminated soil. As demonstrated in Table 3, the CCAN25 had the highest increase in total dry weight (+7%), root length (+5%), stem length (+4%), and leaf area (+45%). CA showed the maximum reduction in total dry weight (−47%), root length (−30%), and leaf area (−43%).

Table 3 The mean comparison of the effect of inoculation of nZVI, cyanobacteria, and AMF individually and repeatedly on the growth parameters of *P. elongata* in contaminated soil

Treatment	Total dry mass	Leaf dry mass (g)	Stem dry mass (g)	Root dry mass (g)	Root length (cm)	Stem diameter (cm)	Leaf area (cm^2)	Colonization (%)
C	251.53 ± 0.76^{B}	31.17 ± 0.95^{B}	208.6 ± 1.37^{B}	11.77 ± 1.59^{B}	57.33 ± 2.15^{B}	276.33 ± 1.53^{B}	11.7 ± 0.5^{CD}	8.44 ± 0.70^{F}
CA	133.77 ± 3.52^{I}	15.47 ± 0.86^{H}	113.17 ± 2.36^{J}	5.13 ± 0.85^{J}	40.13 ± 3.1^{K}	237.64 ± 2.06^{K}	6.66 ± 1.15^{EF}	21.1 ± 0.1^{A}
CC	158.43 ± 0.81^{H}	8.5 ± 0.9^{J}	142.66 ± 0.45^{H}	7.27 ± 0.47^{H}	44.71 ± 4.47^{G}	251.46 ± 1.01^{I}	11.79 ± 1.76^{ABCD}	6.82 ± 0.1^{J}
CN25	168 ± 0.83^{G}	8.13 ± 1.22^{J}	152.67 ± 1.96^{F}	8.03 ± 0.51^{G}	44.14 ± 3.28^{H}	262.51 ± 3.21^{F}	8.77 ± 1.1^{DEF}	7.36 ± 0.4^{I}
CN75	135.9 ± 1.41^{I}	11.5 ± 1.7^{I}	120.83 ± 0.31^{I}	3.57 ± 0.15^{K}	40.7 ± 2.56^{J}	245.93 ± 1.52^{J}	10.53 ± 0.95^{CDE}	7.88 ± 0.5^{G}
CCA	230.3 ± 2.42^{C}	26.53 ± 2.62^{C}	193.4 ± 1.75^{C}	10.36 ± 0.83^{D}	46.33 ± 4.42^{E}	274.67 ± 2.02^{C}	11.52 ± 2.42^{ABC}	18.17 ± 0.42^{C}
CCN25	217.16 ± 4.93^{D}	24.37 ± 3.21^{D}	182.1 ± 2.23^{D}	10.7 ± 0.87^{C}	50.45 ± 3.05^{D}	265.27 ± 2.05^{E}	11.27 ± 2.87^{AB}	7.45 ± 0.6^{H}
CCN75	120.83 ± 1.98^{J}	17.93 ± 1.68^{G}	96.8 ± 0.56^{K}	6.1 ± 0.52^{I}	45.31 ± 7.09^{F}	271.35 ± 2.07^{D}	8.89 ± 0.93^{F}	8.53 ± 0.2^{E}
CCAN25	270.47 ± 2.34^{A}	39.17 ± 3.51^{A}	218.73 ± 1.29^{A}	12.57 ± 0.21^{A}	60.19 ± 2.04^{A}	287.38 ± 2.34^{A}	16.96 ± 0.64^{A}	19.25 ± 0.1^{B}
CCAN75	208.9 ± 3.06^{E}	23.26 ± 2.06^{E}	175.77 ± 0.35^{E}	9.87 ± 0.47^{E}	41.28 ± 6.65^{I}	259.75 ± 1.53^{G}	11.78 ± 1.3^{ABCD}	17.63 ± 0.2^{D}

Different letters indicate statistical significance

Inoculation of microorganisms (AM and cyanobacteria) and nZVI lowered *P. elongata* growth characteristics in contaminated soil. In the case of nZVI, a simultaneous dose of 75 mg/kg combined with other treatments inhibited plant growth, whereas a dose of 25 mg/kg increased it. As a result, the CCAN25 treatment was the only treatment that could significantly boost growth parameters compared to the control sample. These results are consistent with the findings of Zhang et al. (2020). Toxicity is the cause of the decline in growth parameters in treatments with a large amount of NZI, while its low quantity has been able to limit the negative effects of its toxicity and has even increased growth parameters (Mokarram-Kashtiban et al. 2019).

In the case of root colonization by the AM, this percentage is much higher in the mycorrhizal fungus-inoculated treatments than in the other treatments. The largest proportions of colonization in the treatment were CA (+21.01%), CCAN25 (+19.25%), CCA (+18.17%), and CCAN75 (+17.63%), respectively. The percentage of colonization is maximum when mycorrhiza is used separately (CA). If AM was inoculated into a treatment containing cyanobacteria and a dose of 75 mg/kg of iron nanoparticles (CCAN75), the colonization rate was lowered by 16% compared to the control.

Photosynthetic pigments

The photosynthetic pigments (chlorophyll *a*, chlorophyll *b*, and carotenoids) of *P. elongata* in several treatments are shown in Table 4. From this figure, there is a significant difference between all treatments except CCN25 compared to the control.

The largest amount of chlorophyll (+8.5%) was obtained in CCAN25 samples (*P. elongata*), which were subjected to 25 mg/kg NZI, AM, and cyanobacteria. CA treatment (−45%) led to a low amount of chlorophyll in *P. elongata* leaves. CCAN25 treatment was linked to the highest level of chlorophyll *b* (+13.5%) and carotenoids (+12.7%), which is identical to chlorophyll *a*. The lowest amount of chlorophyll *b* (−39%) and carotenoids (42.6%) in the leaves were related to CN75 treatment compared to controls. The trends in chlorophyll *a* and *b* are relatively consistent.

It can also be concluded that the simultaneous presence of AM, cyanobacteria, and NZI resulted in a significant increase in photosynthetic pigments in the plant. In other words, a synergism effect has been observed in treatments with several inoculations while individual application of each has resulted in a significant reduction in photosynthetic pigments in *P. elongata.* Mokarram-Kashtiban et al. (2019) studied the effect of NZI and AM on the phytoremediation of heavy metal–contaminated soil using white willow. They found that increasing the dose of NZI significantly reduces the pigment photosynthetic properties of the plant while AM inoculation had no effect.

Table 4 The mean comparison of photosynthetic pigments in the *P. elongata*

Treatment	Chlorophyll *a*	Chlorophyll *b*	Carotenoids
C	43.91 ± 1.74^{E}	0.74 ± 0.03^{DE}	123.24 ± 0.05^{E}
CA	58.48 ± 0.29^{B}	0.97 ± 0.08^{AB}	185.65 ± 0.13^{BC}
CC	32.12 ± 0.66^{G}	0.70 ± 0.05^{E}	134.10 ± 1.14^{E}
CN25	43.69 ± 1.59^{E}	0.73 ± 0.04^{DE}	172.36 ± 7.76^{D}
CN75	44.68 ± 1.74^{E}	0.88 ± 0.01^{CD}	173.95 ± 4.19^{CD}
CCA	32.32 ± 0.41^{G}	0.59 ± 0.001^{E}	106.54 ± 0.63^{F}
CCN25	53.78 ± 1.42^{CD}	0.90 ± 0.05^{CD}	182.29 ± 3.39^{BCD}
CCN75	56.78 ± 1.41^{BC}	0.95 ± 0.001^{ABC}	209.24 ± 0.04^{A}
CCAN25	34.62 ± 0.79^{F}	0.71 ± 0.06^{DE}	124.75 ± 3.80^{E}
CCAN75	63.42 ± 0.75^{A}	0.74 ± 0.03^{DE}	123.24 ± 0.05^{E}

Different letters indicate statistical significance

Heavy metal concentrations in soil

Chromium(VI)

Figure 3 shows the results of the BCR procedure of Cr(VI) in the soil, 150 days after inoculation with cyanobacteria, AM, and NZI. In form 1 (soluble in acid, exchange, and carbonate), the average concentration of this metal in the control treatment was 0.41 mg/kg. The quantity of this form in all treatment samples was significantly lower than in the control. CCA (−76.5%), CCAN75 (−76%), CN25 (−75%), and CN75 (−73%) treatments showed the highest reductions in control. CCN75 showed the least significant reduction

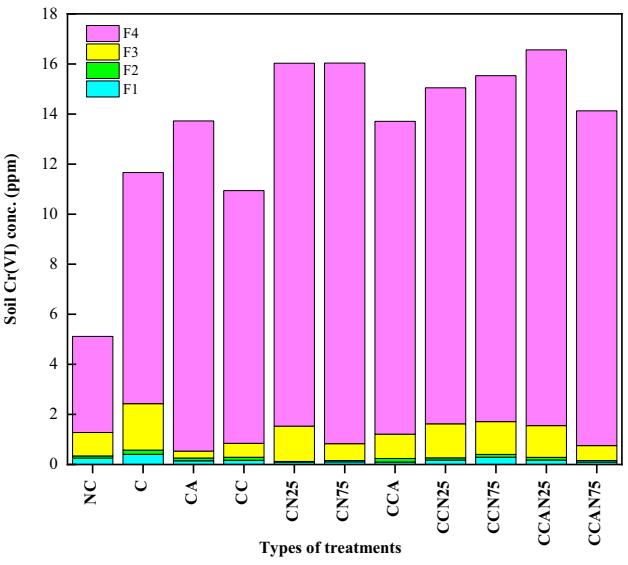

Fig. 3 The Cr(VI) concentration during the four stages of the BCR soil procedure: form 1 (F1), form 2 (F2), form 3, and form 4 (F4)

than control (− 28.4%). These suggest that NZI has a considerable effect in lowering the quantity of form 1 of Cr(VI).

In form 2 (iron–manganese bond), the average concentration of this metal in the control treatment was 0.71 mg/kg. In comparison to the control, all treatments showed a considerable reduction. The highest significant decrease was associated with CN25 treatments (− 86.9%), while the lowest considerable reduction was related to CCA treatments (− 14.3%). Even if the use of AM and cyanobacteria at the same time had the least influence on this form, the percentages of alterations compared to the control reveal that a dose of 25 mg/kg of NZI had a significant effect on it.

In form 3 (oxidation), the average concentration of this metal in the control treatment was 1.85 mg/kg. All treatments led to a significant decrease compared to the control. CA treatment (− 85.2%) showed the highest reduction, while CN25 (− 23.8%) treatment resulted in the lowest substantial reduction in comparison to the control treatment. This indicates that MA individually had the highest effect on the release of this form of Cr(VI) into the soil, whereas the low amount of NZI had the least effect on this form.

In form 4 (residual metals), the average concentration of this metal in the control treatment was 13.2 mg/kg. All treatments showed a significant rise compared to the control. The CN75 (+ 64.6%) had the most significant rise, while the CC treatment (+ 9%) had the least substantial increase. These data suggest that NZI has a considerable impact on residual Cr(VI) in soil, whereas cyanobacteria inoculation separately has the least impact on this type.

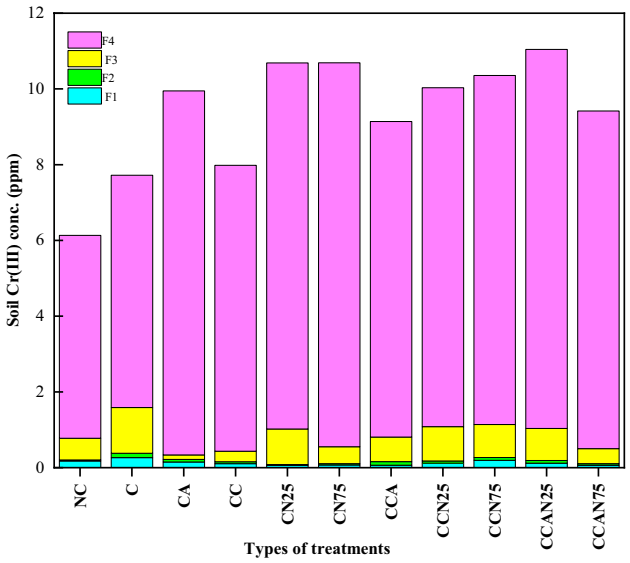

Fig. 4 The Cr(III) concentration during the four stages of the BCR soil procedure: form 1 (F1), form 2 (F2), form 3, and form 4 (F4)

Chromium(III)

Figure 4 illustrates the results of the BCR for Cr(III) in the soil after 150 days of inoculation with cyanobacteria, mycorrhiza, and nZVI, both separately and simultaneously.

In form 1 (acid-soluble, exchangeable, carbonate-bound), the mean concentration of this metal in the control treatment (C) was 0.26 mg/kg. All treatments showed a significant decrease compared to the control at a 0.05 significance level. The highest decrease relative to the control was observed in treatments CCA (− 76%), CCAN75 (− 75.9%), CCAN25 (− 75.4%), and CN75 (− 73.4%). The least significant decrease compared to the control was observed in the CCN75 treatment (− 26.7%). As observed, the trend of changes in this form for trivalent chromium was similar to hexavalent chromium. This indicates that cyanobacteria can only be effective in reducing the availability of this metal if used either simultaneously with mycorrhiza or simultaneously with iron nanoparticles.

In form 2 (iron–manganese bond), the mean concentration of this metal in the control treatment (C) was 0.11 mg/kg. The highest significant decrease was observed in treatments CN25 (− 87.3%) and CN75 (− 71.1%). The least significant decrease was associated with the CCA treatment (− 16.7%). These numbers indicate that iron nanoparticles can effectively reduce Cr(III) in this form (reducing its bond with iron–manganese) when used separately. However, mycorrhiza and cyanobacteria, contrary to their significant role in form 1, were not very effective.

In form 3 (oxidizable), the mean concentration of this metal in the control treatment (C) was 1.21 mg/kg. All treatments showed a significant decrease compared to the control. The highest decrease relative to the control was associated with the CA treatment (− 90%), and the least significant decrease was observed in the CN25 (− 22.1%), CCN25 (− 25.1%), CCN75 (− 27.2%), and CCN25 (− 30%) treatments. These numbers indicate that AMF's effect compared to iron nanoparticles is more significant in releasing Cr(III) into the soil under oxidizing conditions.

In form 4 (residual metals), the mean concentration of this metal in the control treatment (C) was 13.2 mg/kg. All treatments showed a significant increase compared to the control. The highest significant increase relative to the control was observed in the CN75 treatment (+ 65.3%), followed by the CCAN25 (+ 63.2%) and CN25 (+ 57.6%) treatments. The lowest increase was associated with the CC treatment (+ 23%). These variations indicate that a significant portion of trivalent chromium is bound to mineral networks and crystalline oxides. In addition, it can be said that its accessibility to plants has decreased in treatments containing iron nanoparticles, whereas cyanobacteria did not have a noticeable effect on this form.

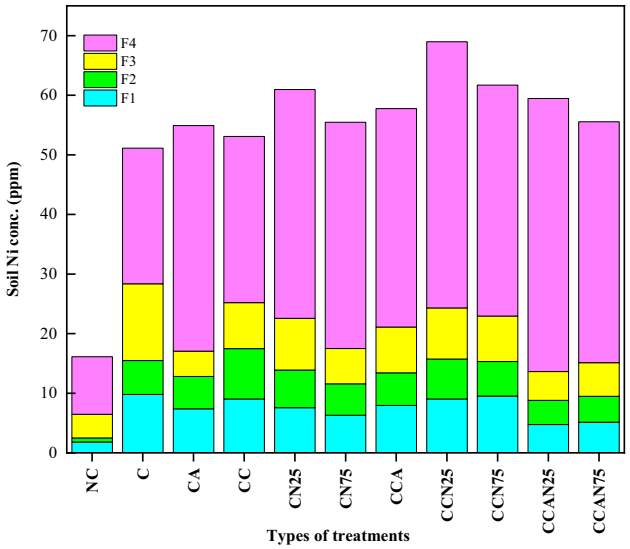

Fig. 5 The nickel concentration during the four stages of the BCR soil procedure: form 1 (F1), form 2 (F2), form 3, and form 4 (F4)

Nickel

Figure 5 represents the result of the BCR indicating the concentration of Ni in the soil after 150 days from the start of inoculation with cyanobacteria, mycorrhiza, and nZVI separately and simultaneously.

In form 1 (acid-soluble, exchangeable, carbonate), the average concentration of this metal in the control treatment (C) was 9.8 mg/kg. All treatments showed a significant decrease compared to the control at the 0.05 level. The highest reduction compared to the control was observed in treatments CCAN25 (−51.4%) and CCAN75 (−47.6%), respectively. The least significant decrease compared to the control was observed in treatment CCN75 (−2.8%). These variations indicate that the simultaneous use of all amendments had a noticeable effect on reducing this form (acid-soluble, exchangeable, carbonate), while the separate or simultaneous use of iron nanoparticles did not result in a significant reduction when used in conjunction with cyanobacteria.

In form 2 (iron–manganese oxide bond), the average concentration of this metal in the control treatment (C) was 5.7 mg/kg. All treatments showed a significant decrease compared to the control at the 0.05 level. The highest reduction compared to the control was observed in treatments CC (−48%) and CCN25 (−17.9%), respectively. The least significant decrease compared to the control was observed in treatments CCAN25 (−28.2%) and CCAN75 (−23.4%). These variations indicate that the highest reduction in this form occurred when all amendments were used simultaneously. In addition, a significant increase occurred when treatments included cyanobacteria (separately).

In form 3 (oxidizable), the average concentration of this metal in the control treatment (C) was 12.9 mg/kg. The highest reduction compared to the control was observed in treatment CA (−67.1%), and the least significant decrease compared to the control was observed in treatments CCN25 (−33.3%) and CN25 (−32.7%). This indicates that mycorrhiza had the most significant impact on reducing the nickel bond with organic soil materials. In addition, a small amount of iron nanoparticles did not have a significant effect on this form.

In form 4 (residual metals), the average concentration of this metal in the control treatment (C) was 22.7 mg/kg. All treatments showed a significant increase compared to the control. The highest significant increase compared to the control was observed in treatments CCAN25 (+101.4%) and CCN25 (+96.3%), respectively. The lowest increase was observed in treatment CC (+22.6%). These variations indicate that a major portion of nickel was bound to mineral networks and crystalline oxides. It can also be said that a small number of iron nanoparticles had a considerable effect on increasing this form (reducing further accessibility and mobility of nickel), while cyanobacteria (separately) did not have a noticeable effect compared to other amendments.

Heavy metal concentrations in plant

Chromium(VI)

Figure 6 illustrates the absorbed amounts of Cr(VI) by *P. elongata* leaves under different treatments. The concentration of Cr(VI) in *P. elongata* leaves in treatment C (control) was measured at 1.01 mg/kg. The highest significant increase in adsorption compared to treatment C was observed in treatments CCN25 with a value of 1.52 mg/kg (+50%), CA with a value of 1.19 mg/kg (+17%), and CN75 with a value of 1.17 mg/kg (+15%). In addition, treatment CCN75 exhibited the highest significant decrease compared to treatment C, with an adsorption value of 0.92 mg/kg (−9%).

Figure 6 illustrates the absorbed amounts of Cr(VI) by the stem of *P. elongata* under different treatments. The concentration of Cr(VI) in *P. elongata* stem in treatment C was measured at 0.95 mg/kg. The highest significant increase in adsorption compared to treatment C was observed in treatments CA with a value of 1.73 mg/kg (+23%) and CC with a value of 1.08 mg/kg (+14%). In addition, treatment CCAN75 exhibited the highest significant decrease compared to treatment C, with an absorbed value of 0.56 mg/kg (−41%).

Figure 6 demonstrates the absorbed amounts of Cr(VI) by the roots of *P. elongata* under different treatments. The concentration of Cr(VI) in *P. elongata* roots in treatment C was measured at 1.62 mg/kg. The highest significant increase in adsorption compared to treatment C was observed in

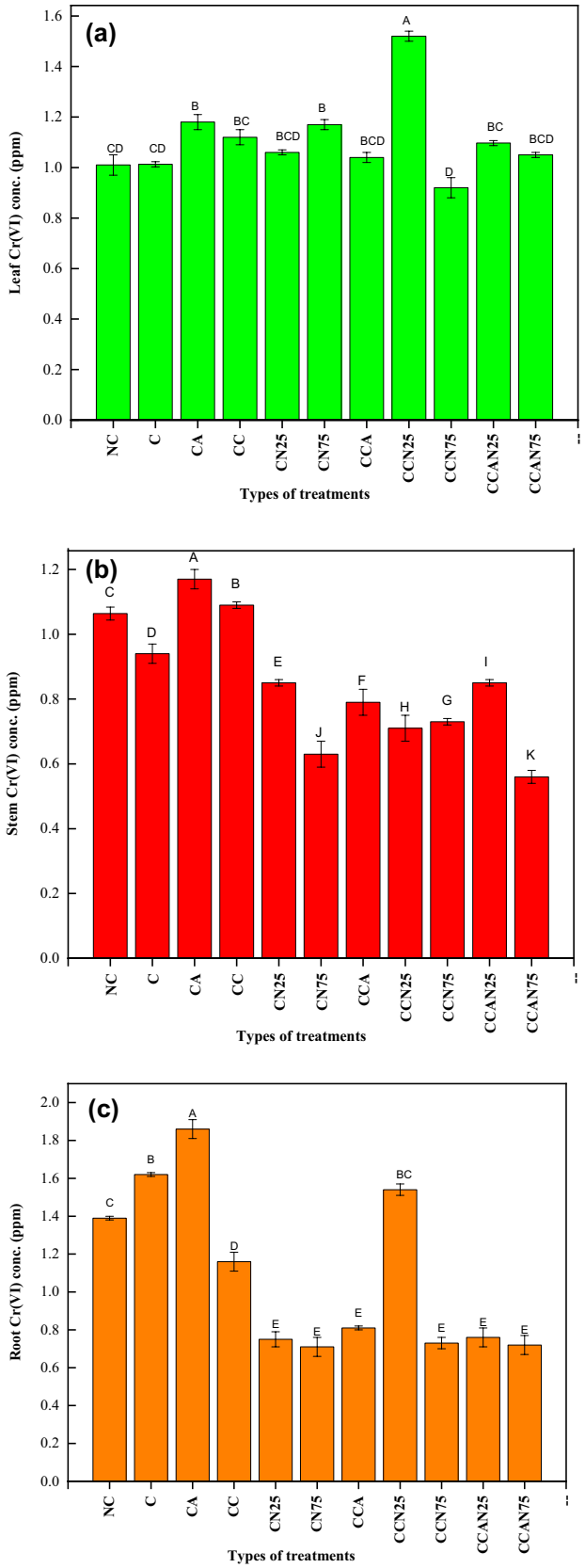

Fig. 6 The concentration of Cr(VI) in the leaves (**a**), stem (**b**), and roots (**c**) of *P. elongata*. Different letters indicate statistical significance

treatment CA with a value of 1.86 mg/kg (+15%) (the only treatment that showed an increase compared to the control). Furthermore, in descending order (as shown in the figure below, indicating that these six treatments do not significantly differ from each other), the adsorption values for treatments CN75 were 0.71 mg/kg (−56%), CCAN75 was 0.72 mg/kg (−5.55%), CCN75 was 0.73 mg/kg (−9.54%), CN25 was 0.75 mg/kg (−5.53%), CCAN25 was 0.76 mg/kg (−1.53%), and CCA was 0.81 mg/kg (−50%), showing the highest significant decrease compared to treatment C.

Chromium(III)

Figure 7 illustrates the absorbed amount of Cr(III) by the leaves of the *P. elongata* under different treatments. The concentration of Cr(III) in *P. elongata* leaves in treatment C was measured at 2.03 mg/kg. The highest significant increase in adsorption compared to treatment C was observed in treatments CN25 with a value of 0.82 mg/kg (+6.36%), CCN75 with a value of 0.72 mg/kg (+7.33%), and CCA with a value of 0.62 mg/kg (+30%). In addition, treatment CN75 exhibited the highest significant decrease compared to treatment C, with an adsorption value of 0.65/1 mg/kg (−5.18%).

Figure 7 demonstrates the absorbed quantity of Cr(III) by the stems of the *P. elongata* under different treatments. The concentration of Cr(III) in *P. elongata* stems in treatment C was measured at 1.38 mg/kg. The highest significant increase in adsorption compared to treatment C was observed in treatments CN25 with a value of 1.3 mg/kg (+7.122%), CCAN75 with a value of 0.42 mg/kg (+48%), and CCA with a value of 0.92 mg/kg (+39%). In addition, treatment CCN75 exhibited the lowest significant increase compared to treatment C, with an adsorption value of 0.561 mg/kg (+13%).

Figure 7 illustrates the adsorption amount of Cr(III) by the roots of *P. elongata* under different treatments. The concentration of Cr(III) in *P. elongata* roots in treatment C was measured at 7.7 mg/kg. The highest significant increase in adsorption compared to treatment C was observed in treatments CN25 with a value of 11.7 mg/kg (+50%), CCA with a value of 11.6 mg/kg (+45%), and CN75 with a value of 11.02 mg/kg (+43%). In addition, treatment CCN75 exhibited the highest significant decrease compared to treatment C, with an adsorption value of 4.47 mg/kg (−42%).

Nickel

Figure 8 demonstrates the adsorption capacity of Ni by the leaves of *P. elongata* under different treatments. The concentration of Ni in *P. elongata* leaves in treatment C was measured at 8.57 mg/kg. The highest significant increase in adsorption compared to treatment C was observed in treatments CC with a value of 15.18 mg/kg (+77%), CCN25

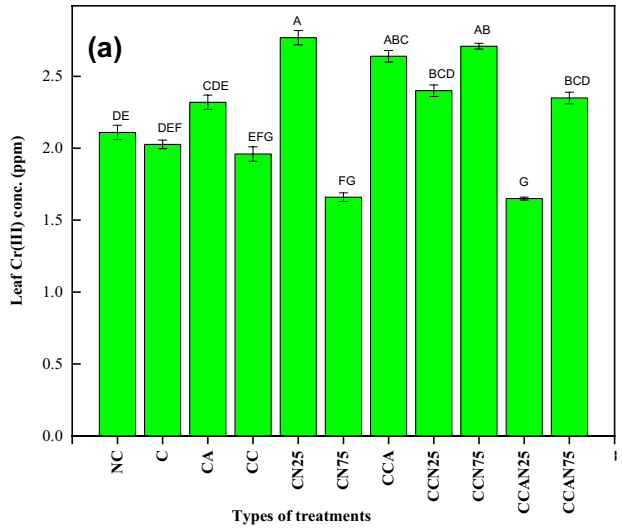

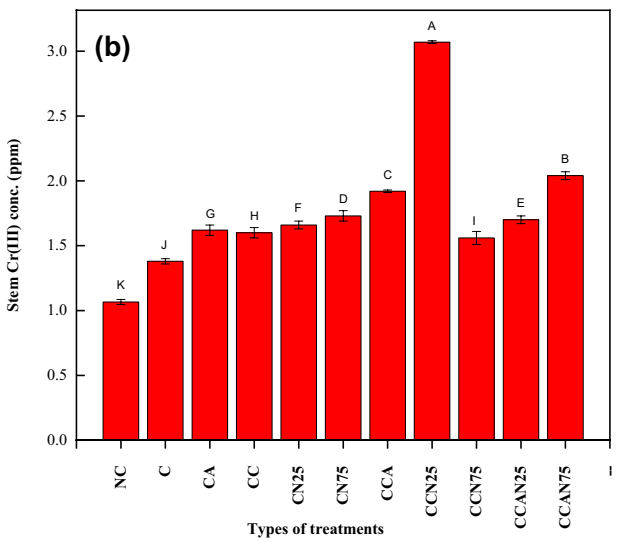

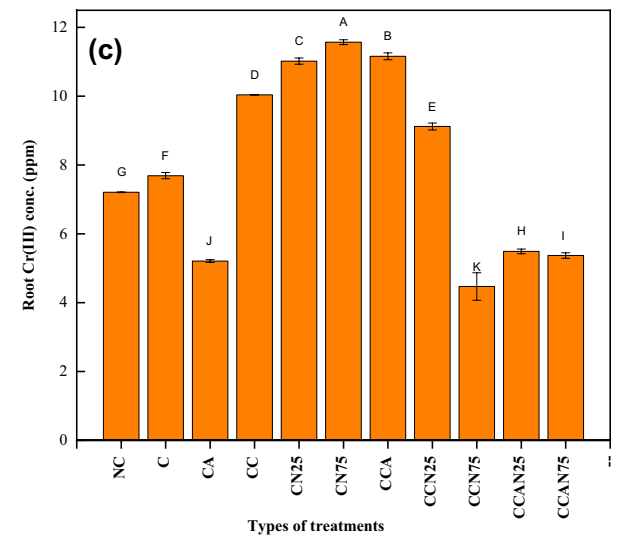

Fig. 7 The concentration of Cr(III) in the leaves (**a**), stem (**b**), and roots (**c**) of the *P. elongata* plant. Different letters indicate statistical significance

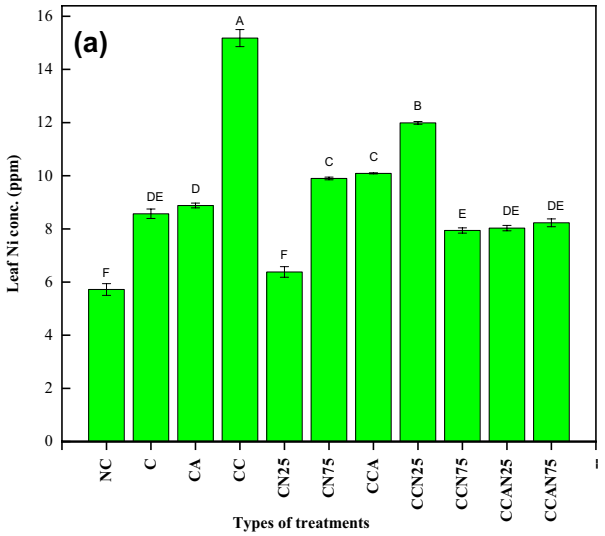

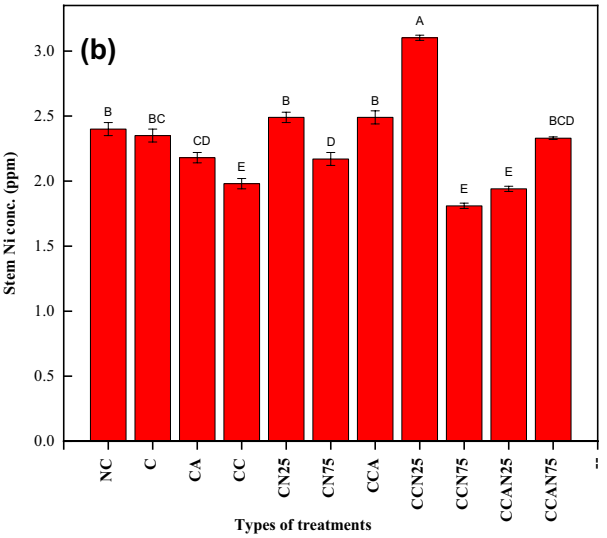

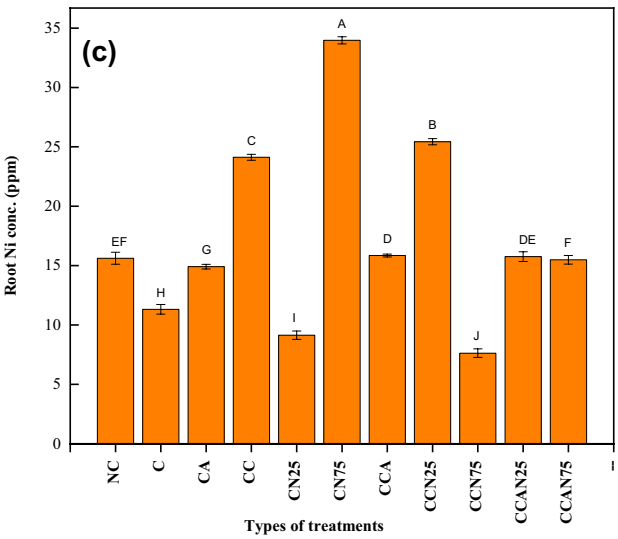

Fig. 8 The concentration of nickel in the leaves (**a**), stem (**b**), and roots (**c**) of the *P. elongata* plant. Different letters indicate statistical significance

with a value of 11.99 mg/kg (+40%), and CCA with a value of 10.09 mg/kg (+17%). In addition, treatment CN25 exhibited the highest significant decrease compared to treatment C, with an adsorption value of 6.38 mg/kg (−25%).

Figure 8 illustrates the adsorption amount of Ni by the stems of *P. elongata* under different treatments. The concentration of Ni in *P. elongata* stems in treatment C was measured at 2.35 mg/kg. The highest significant increase in adsorption compared to treatment C was observed in treatments CCN25 with a value of 3.10 mg/kg (+31%), CCA with a value of 2.49 mg/kg (+6%), and CN25 with a value of 47.2 mg/kg (+5%). In addition, treatment CCN75 exhibited the highest significant decrease compared to treatment C, with an adsorption value of 1.81 mg/kg (−23%).

Figure 8 presents the adsorption capacity of Ni by the roots of *P. elongata* under different treatments. The concentration of Ni in *P. elongata* roots in treatment C was measured at 11.32 mg/kg. The highest significant increase in adsorption compared to treatment C was observed in treatments CN75 with a value of 33.97 mg/kg (+200%), CCN25 with a value of 11.4 mg/kg (+124%), and CC with a value of 24.12 mg/kg (+113%). In addition, treatment CCN75 exhibited the highest significant decrease compared to treatment C, with an adsorption value of 7.63 mg/kg (−32%).

Phytoremediation efficiency of P. elongata

To determine the phytoremediation efficiency of *P. elongata* for heavy metal remediation, the concentrations of heavy metals in different parts of the plant (roots, stems, and leaves) and soil were measured. Then, by calculating indices such as TI (tolerance index), TF (transfer factor), BCF (bioaccumulation factor in roots), and BAC (bioaccumulation factor in shoots), the capability and efficiency of the plant for phytoremediation can be assessed.

Tolerance index

Figure 9 illustrates the tolerance index of *P. elongata* for Cr and Ni. According to this table, the tolerance index in the control treatment is equal to 1. However, this index was higher than the control treatment only in the CCAN25 treatment (with a value of 1.07). This indicates that the use of a low amount of iron nanoparticles in conjunction with mycorrhiza and cyanobacteria can enhance the plant's tolerance to high stresses. It should be noted that the lowest decrease in the tolerance index was observed in the CCA treatment (with a value of 0.91), while the highest decrease compared to the control was related to the CCN75 treatment (with a value of 0.48). These numbers indicate that the use of a high concentration of iron nanoparticles can be considered a stress factor. In addition, the simultaneous use of mycorrhiza and cyanobacteria can partially compensate for the negative effects of stress on plant tolerance. It is good to mention that the tolerance index is approximately 1 when the plant is under no stress, and this value decreases toward 0 when the plant is exposed to pollutants. This index represents the ratio of the plant's dry weight in treatment to the plant's dry weight in the control (Cao et al. 2008; Mokarram-Kashtiban et al. 2019).

Transfer factor

Figure 10 shows the translocation index of *P. elongata* for Cr and Ni. The translocation index for Cr in the control

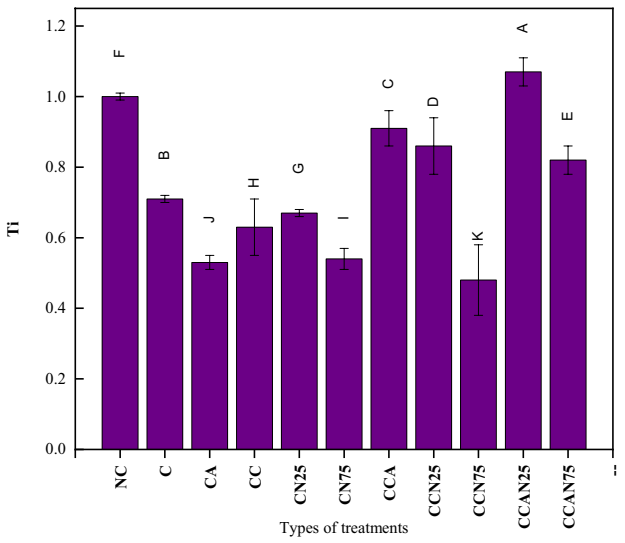

Fig. 9 TI in *P. elongata* for heavy metal phytoremediation

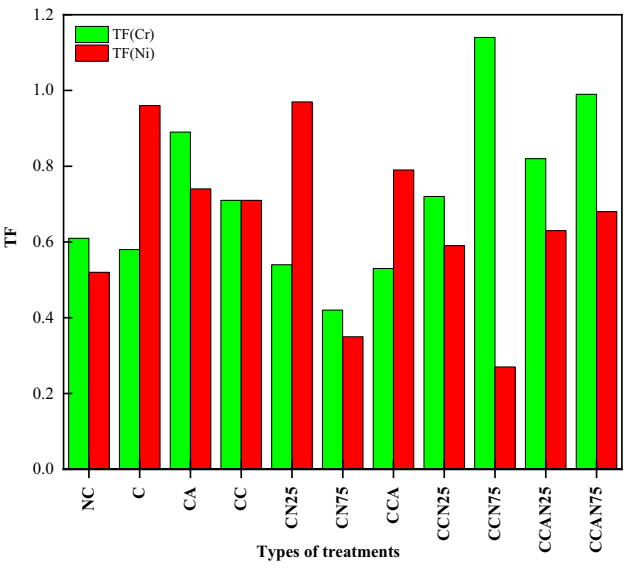

Fig. 10 TF in *P. elongata* for heavy metal phytoremediation

treatment is 0.57, while the CCN75 treatment (1.41) has the highest value, and the CN75 treatment (0.42) has the lowest value. This means that cyanobacteria have significantly increased the translocation of Cr from the soil to the aerial parts of the plant. In addition, it can be inferred that a high concentration of iron nanoparticles (separately) has significantly reduced this index for Cr. The translocation index for Ni in the control treatment is 0.96, while the CCN75 treatment (1.27) has the highest value, and the CN75 treatment (0.35) has the lowest value. Similar to Cr, cyanobacteria have significantly increased the translocation of Ni from the soil to the aerial parts of the plant, and the separate use of a high concentration of iron nanoparticles has resulted in the most significant reduction in this index.

This index indicates the ability of heavy metal translocation from the roots to the aerial parts (stem and leaves) of the plant. If the translocation index for a metal is less than 1, its absorption and translocation to the shoot (stem and leaves) are limited. Generally, a higher value of this index means that the metal has been transferred more from the soil to the plant. It has been mentioned that when the translocation index is less than 1, the plant is considered an accumulator, and when it is greater than 1, the plant is a hyperaccumulator for that metal. The translocation index is used to determine the metal's mobility because it is derived from the ratio of metal concentration in the shoot (stem and leaves) to the metal concentration in the soil (Mokarram-Kashtiban et al. 2019).

Bioconcentration factor

Figure 11 illustrates the phytoaccumulation index of *P. elongata* for Cr and Ni. The phytoaccumulation index for Cr in the control treatment is 1.41. In comparison, the CN75 treatment has the highest value (1.50), while the CCN75 treatment has the lowest value (0.64). Similarly, the phytoaccumulation index for Ni in the control treatment is 0.39, with the CN75 treatment having the highest value (1.17) and the CCN75 treatment having the lowest value (0.26). In general, the CN75 treatment has achieved the highest phytoaccumulation (root) for Cr and Ni. This means that the use of a high amount of iron nanoparticles (separately) has led to higher phytoaccumulation of these three metals in the roots compared to other treatments. Conversely, the CCN75 treatment has resulted in the lowest phytoaccumulation (root) for both of them. This implies that the simultaneous use of a high amount of iron nanoparticles and cyanobacteria imposes the greatest limitation on the phytoaccumulation of these four metals.

Bioaccumulation coefficient

Figure 12 displays the phytoaccumulation index of the *P. elongata* for Cr and Ni. The bioaccumulation factor for Cr in the control treatment is 0.65, while the CCN25 treatment has the highest value (0.94), and the CCAN25 treatment has the lowest value (0.34). In addition, the bioaccumulation factor for Ni in the control treatment is 0.37, with the CC treatment having the highest value (0.59) and the CN25 treatment having the lowest value (0.31). In general, only the CCN25 treatment (with a value of 0.42) has a phytoaccumulation index greater than 1. This means that the simultaneous use of cyanobacteria and iron nanoparticles has led to a high phytoaccumulation of iron. On the other hand, the lowest phytoaccumulation in the shoots for iron is related to

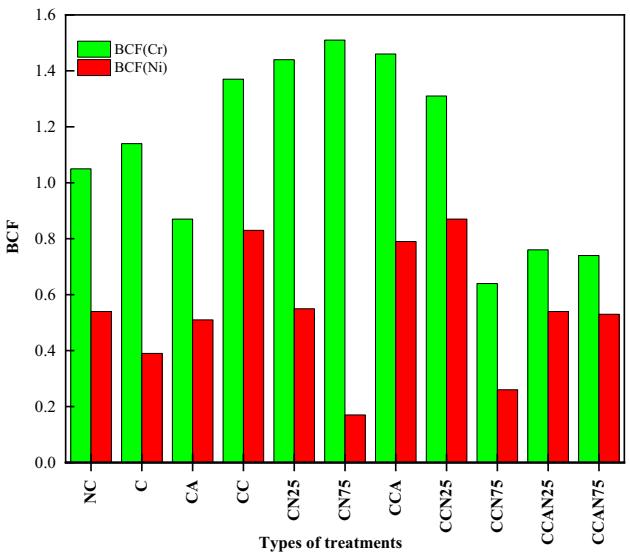

Fig. 11 BCF in *P. elongata* for heavy metal phytoremediation

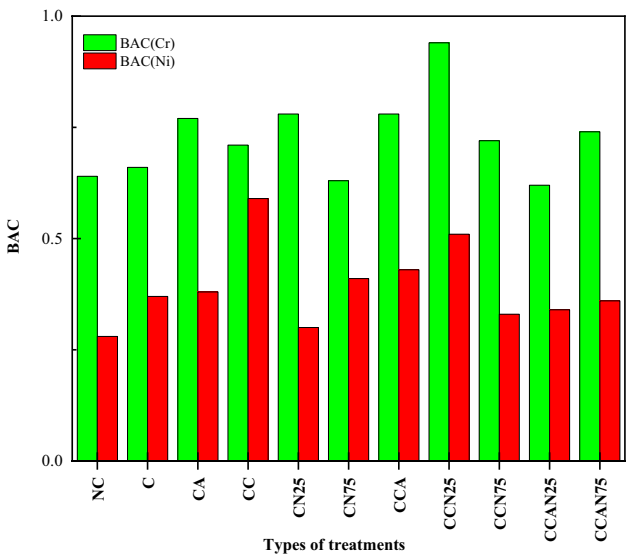

Fig. 12 BAC in *P. elongata* for heavy metal phytoremediation

the CCA treatment (simultaneous use of cyanobacteria and mycorrhiza) with a value of 0.14.

A 4-degree scale is used to assess metal phytoaccumulation. If the bioconcentration factor (BCF) or bioaccumulation coefficient (BAC) is less than 0.01, there will be no phytoaccumulation of that metal in the plant. If it is between 0.01 and 0.1, phytoaccumulation is low. If it is between 0.1 and 1.0, phytoaccumulation is moderate. If it is greater than 1.0, phytoaccumulation is high (Sekabira et al. 2011). Based on this, in our study, the BCF and BAC values for both metals were less than 1.0, indicating moderate phytoaccumulation of Cr and Ni in *P. elongata* (across all treatments). It can also be concluded that the simultaneous use of cyanobacteria and mycorrhiza resulted in the highest phytoaccumulation of Cr in the roots (BCF), while the opposite effect was observed when a high amount of iron nanoparticles was used in addition to cyanobacteria and AMF (Yoon et al. 2006). By comparing BCF and BAC, we can determine in which plant tissue the metal has a higher phytoaccumulation. In general, the higher the values of these two indices, the greater the plant's ability to accumulate heavy metals.

Synergistic effects of amendments on the phytoremediation process

In general, as expected, a synergistic effect was observed in the phytoremediation process when remediation amendments (cyanobacteria, AMF, and nZVI) were used simultaneously. In the treatment of CCAN25 (ternary), the photosynthetic pigments (chlorophyll *a* and *b*) in leaves and growth parameters (total dry weight, stem length, root length) exhibited the highest values. On the other hand, the concentrations of metals, including Cr(VI) and Ni, were the lowest in both the plants and soil in the ternary treatment.

Discussion

Effect of cyanobacteria inoculation on the phytoremediation process

Cyanobacteria play a crucial role in tackling environmental pollution caused by rapid industrialization and urbanization. They are key players in environmental biotechnology, leading efforts for ecological restoration. Cyanobacteria's distinct benefits, such as rapid metal removal, microbial biomass capacity for extracting metallic ions, and reliance on natural biomaterials, make them superior to traditional methods. Thriving across soil systems, cyanobacteria demonstrate a remarkable capacity to accumulate significant levels of metals (Gupta et al. 2012).

The study observed that cyanobacteria significantly reduced the EC of the soil. Kheirfam and Roohi (2020) observed that cyanobacteria reduce soil EC by absorbing sodium through algal biomass. Algae in the soil, particularly during rainy days (in high moisture conditions), use sodium instead of calcium, resulting in reduced electrical conductivity. Besides, Singh and Singh (2015) studied the impact of cyanobacteria on saline and alkaline soils, observing a reduction in soil EC from 5.6 to 6.5 dS/m after 3 months. Al-Sherif et al. (2015b) found that cyanobacteria significantly reduced the soil EC by up to 80% in the bioremediation of heavy metal-contaminated soils. In addition, Nisha et al. (2018) demonstrated cyanobacteria's capacity to lower soil EC.

Cyanobacteria, with their ability to fix atmospheric nitrogen and carbon, emerge as fitting candidates for bioremediation (Gupta et al. 2012; Ramakrishnan et al. 2023). In this study, the inoculation of cyanobacteria led to a significant increase in soil organic carbon and nitrogen levels, while also enhancing phosphorus and potassium levels through photosynthesis. Cyanobacteria, through photosynthesis, can increase the organic carbon and nitrogen content of the soil (Kheirfam and Roohi 2020). The fixation of nitrogen by cyanobacteria substantially enhances the availability of this crucial nutrient in the soil. Furthermore, cyanobacteria play a pivotal role in preserving nitrogen, phosphorus, organic carbon, and soil moisture, as elucidated by Chittora et al. (2020). Numerous studies have delved into the diverse impacts of cyanobacteria on different soil types. For example, Singh and Singh (2015) found that cyanobacteria significantly increased organic carbon in saline and alkaline soils. Román et al. (2018) studied the interactions between algae, bacteria, and the environment, and found that cyanobacteria increased both organic carbon and nitrogen in the soil. Al-Sherif et al. (2015a) investigated the bioremediation of heavy metal–contaminated soils and reported significant increases in nitrogen and phosphorus after cyanobacteria inoculation. In contrast, Biglari Quchan Atigh et al. (2020) studied native cyanobacteria in heavy metal–contaminated soils and observed a reduction in soil nitrogen and organic carbon following cyanobacteria inoculation.

Cyanobacteria, equipped with the capability to fix atmospheric nitrogen and carbon, emerge as ideal candidates for bioremediation within the realm of heavy metals, encompassing vital micronutrients and harmful elements (Ramakrishnan et al. 2023). In this study, the presence of cyanobacteria in soil treated with cyanobacteria resulted in a significant decrease in the concentration of metals such as Cr(VI) compared to the control. Microorganisms, acting as catalysts, can efficiently convert Cr(VI) to less toxic Cr(III). This bioremediation process can effectively reduce the mobility of Cr(VI) in the soil (Chittora et al. 2020). Studies by Biglari Quchan Atigh et al. (2020) and Al-Sherif et al. (2015b) observed substantial reductions in various heavy metals after cyanobacteria inoculation in

soils, demonstrating their effectiveness in remediating metal-contaminated sites. Some cyanobacteria possess special polysaccharide sheaths around cell walls, which not only protect cells from oxygen but also enhance water absorption capacity, moisture retention, microbial activity, and the accumulation of biologically derived elements (Kheirfam and Roohi 2020). Bioflocculants, synthesized extracellular macromolecules by cyanobacteria, play a pivotal role in efficiently removing heavy metals from contaminated sites by binding and sequestering them, contributing to their multifaceted role in bioremediation (Gupta et al. 2012).

Cyanobacteria play a vital role in enhancing plant tolerance and protection through a sophisticated mechanistic process (Abo-Shady et al. 2023). In this work, when cyanobacteria was applied to *P. elongata* in contaminated soil, it led to an increase in both the tolerance index (TI) and the translocation index (TF). This elevation in TI and TF is associated with the positive effects of cyanobacteria, potentially mitigating stress induced by heavy metals. The mechanisms contributing to enhanced plant tolerance include biosorption, bioflocculation, and cyanobacteria's role in soil improvement. Moreover, cyanobacteria, in symbiosis with plants, effectively mitigate the adverse impacts of abiotic stresses and heavy elements, significantly contributing to the biogeochemical cycles of nitrogen, carbon, and oxygen in the soil (Poveda 2021).

Effect of mycorrhiza on the phytoremediation process

AMF exhibits considerable variability in resistance to heavy metals. In this study, the introduction of AMF led to a noteworthy decrease in the concentrations of Cr and Ni in forms I, II, and III, in comparison to the control treatment. AMF detoxifies metal contamination through surface adsorption and soil immobilization by glomalin (Vilela and Barbosa 2019). AMF releases glomalin-related soil protein (GRSP) in the form of low molecular weight organic compounds. GRSP, produced by AMF through mycelium and spore walls, exhibits water insolubility and temperature resistance, serving a crucial role in metal chelation in the rhizosphere (Riaz et al. 2021). This is possibly linked to the decline in metal concentration in phase III in this study, representing the oxidized form (bound with organic sulfides), implying low bioavailability and mobility due to association with sulfur and high molecular weight organic materials. This form releases minimal metals into the environment gradually.

AMF plays a crucial role in enhancing plant biomass and metal tolerance, influencing heavy metal (HM) bioavailability, and promoting HM retention in roots. While some AMF strains restrict HM translocation to aerial parts, others enhance HM uptake. In this study, AMF inoculation into the soil significantly reduced the photosynthetic pigments (chlorophyll *a* and *b*) in the leaves of *P. elongata* plants, as well as the total dry weight, stem length, root length, and leaf surface area. On the other hand, a notable decrease in the bioconcentration factor (BCF) for Cr was observed, accompanied by an increase in BCF for Ni. Furthermore, it is noteworthy that the translocation factor (TF) for Ni showed a decrease.

Several studies have investigated the effects of AMF on plant growth and metal toxicity. Citterio et al. (2005) observed a reduction in plant biomass due to metal accumulation in the roots. Mycorrhizal plants consume more energy, relying on the plant for carbon supply, and if carbon production is insufficient, the plant's energy consumption by the fungus becomes apparent, resulting in decreased biomass. Chen et al. (2005) observed a significant increase in lead accumulation in the aerial parts and roots of *Kummerowia striata* Thunb., *Ixeris denticulate* Houtt., *Lolium perenne* L., and *Trifolium repens* L. plants due to AMF symbiosis. Furthermore, Killham and Firestone (1983) noted that symbiosis does not consistently boost plant growth and may adversely affect certain growth parameters. Their study found increased heavy metal concentrations in the roots and aerial parts of mycorrhizal herbaceous plants compared to non-mycorrhizal ones. Elevated heavy metal levels can disrupt crucial metabolic activities like photosynthesis, enzyme function, and hormone regulation in plants. AMF plays a pivotal role in assisting plants in coping with heavy metals. They induce alterations in plant morphology and physiology, enhancing the plant's resilience to HM stress. AMF produces chelators that impede the translocation of metals to the upper parts of the plant, thereby augmenting the plant's capacity to manage HMs. The extraradical hyphae of AMF exhibit robust metal-binding capabilities, contributing to effective phytoremediation. The cell walls of AMF contain compounds such as chitin and chitosan, influencing HM binding strength through specific amino acids. In addition, plants associated with AMF benefit from fungal threads in the soil, producing glomalin. In essence, AMF supports plants in tolerating metals by capturing and immobilizing them effectively (Riaz et al. 2021).

Effect of NZI on the phytoremediation process

The results of this study show that the addition of nZVI at both concentrations (25 and 75 mg/kg) did not significantly affect the pH, but it significantly increased the EC (higher nanoparticle concentration resulted in a greater increase). Since nZVI can retain or absorb ions present in the soil, the increase in EC with increasing iron nanoparticle concentration can be attributed to this reason (Wong et al. 2007). In addition, iron inoculation into the soil itself leads to an increase in EC (Hidalgo et al. 2020). The findings of several studies conducted by Mokarram-Kashtiban

et al. (2019), Pavelková et al. (2021), and Song et al. (2019) confirm our study results.

Our finding showed that the treatment with higher nZVI (75 mg/kg) caused a significant decrease in the concentrations of Cr in forms 1, 2, and 4 in the soil, while lower nZVI (25 mg/kg) resulted in a significant decrease in forms 1, 2, and 3. Regarding Ni, a significant reduction was observed in form 3 in the treatment where a low dose of nanoparticles was used. nZVI is thoroughly investigated for its efficacy in pollutant removal through redox reactions. Functioning as an electron donor, nZVI facilitates the reductive degradation or stabilization of pollutants, particularly Cr(VI). Beyond its reducing capabilities, nZVI can also adsorb inorganic ions and coprecipitate with them (Song et al. 2019). The nZVI has a core made of zero-valent iron, also known as metallic iron, while they have an oxide shell resulting from the oxidation of metallic iron. The core can lose electrons. Metals with a more positive standard electrode potential (E°) than iron (-0.89 V), such as Cr (-0.74 V) and Ni (-0.25 V), are removed both through the process of electron transfer from iron to the metal and through surface adsorption (Tafazoli et al. 2020).

The photosynthetic pigments (chlorophyll *a* and *b*) experienced a significant reduction compared to the control as a result of this inoculation. Growth and biometric indices in the *P. elongata* also showed a significant decrease due to this inoculation. It is noteworthy that following this inoculation at a dosage of 75 mg/kg, there was a significant reduction in Cr(VI) concentrations in the leaves, stem, and roots of *P. elongata*. However, the concentrations of Cr(III) increased in the stem and roots. As for Ni, its concentration elevated in the leaves and roots of *P. elongata*. Furthermore, the BCF exhibited an augmentation for Cr and a reduction for Ni at a dosage of 75 mg/kg. In addition, the TF demonstrated a decline for both Cr and Ni in comparison to the control group at the abovementioned dose. Mokarram-Kashtiban et al. (2019) noted that the introduction of iron nanoparticles into heavy metal–contaminated soil impacts growth parameters, resulting in a reduced TF and BCF for cadmium and lead at lower nZVI doses. Hidalgo et al. (2020) found that the introduction of nZVI facilitated the movement of pollutants to the aboveground parts of the plant, while plant tolerance remained unaffected. The efficacy of nZVI in capturing metal(loid)s is contingent on their unique characteristics, and there may be a competitive interaction among different metal(loid)s. Cr, having a slightly higher E° than Ni, can be more effectively immobilized by nZVI through sorption and precipitation. This could be a contributing factor to why nZVI led to a reduction in root accumulation of Cr concentration.

Conclusion

This study investigated the individual and combined effects of cyanobacteria, AMF, and nZVI in conjunction with *P. elongata* for remediating soil contaminated with Cr and Ni. The results indicated that cyanobacteria, either alone or in combination with AMF and nZVI, significantly reduced EC. Nitrogen content varied across treatments, with the combined application of cyanobacteria and AMF showing the most significant increase. Significant variations in phosphorus content were observed, particularly in the treatment involving cyanobacteria, AMF, and a high amount of nZVI. The highest increase in potassium content was observed in the cyanobacteria and high nZVI treatment. The organic carbon content of the soil increased significantly in the treatment with cyanobacteria, a low amount of nZVI, and AMF, while the presence of 75 mg/kg of nZVI led to a decrease. Plant growth metrics showed significant differences in all treatments, with the treatment involving cyanobacteria, nZVI, AMF, and a low amount of nZVI resulting in the highest plant growth. In addition, the combined application of cyanobacteria, nZVI, AMF, and a low amount of nZVI exhibited the highest levels of chlorophyll *a*, chlorophyll *b*, and carotenoids. BCF and BAC values suggested moderate phytoaccumulation of Cr and Ni in *P. elongata* across all treatments, with the highest phytoaccumulation of Cr in roots observed in the CCAN25 treatment. In conclusion, the simultaneous application of cyanobacteria, AMF, and nZVI demonstrated significant effects on soil properties, plant growth, and heavy metal availability, highlighting their potential for remediating Cr- and Ni-contaminated soil.

Acknowledgements The authors thank the Ferdowsi University of Mashhad for providing financial support for conducting this project.

Author contribution Sara Khoshyomn: software, formal analysis, investigation, resources, data curation, writing—original draft, visualization, funding acquisition. Ava Heidari: conceptualization, methodology, software, validation, investigation, resources, data curation, writing—original draft, writing—review and editing, visualization, supervision, funding acquisition, project administration. Mohammad Farzam: methodology, software. Zeinab Shariatmadari: methodology. Zahra Karimian: methodology, validation, software, writing—review and editing.

Funding This study was funded by the Ferdowsi University of Mashhad (51035) of Iran.

Declarations

Conflict of interest The authors declare no competing interests.

References

Abo-Shady AM, Osman ME-AH, Gaafar RM, Ismail GA, El-Nagar MMF (2023) Cyanobacteria as a valuable natural resource for improved agriculture, environment, and plant protection. Water Air Soil Pollut 234(5):313

Ahemad M, Khan MS (2012) Effect of fungicides on plant growth promoting activities of phosphate solubilizing Pseudomonas putida isolated from mustard (Brassica compestris) rhizosphere. Chemosphere 86(9):945–950

Al-Sherif EA, Ab El-Hameed M, Mahmoud MA, Ahmed HS (2015a) Use of cyanobacteria and organic fertilizer mixture as soil bioremediation. Am-Eurasian J Agric Environ Sci 15:794–799

Al-Sherif EA, Abd El-Hameed MS, Mahmoud MA, Ahmed HS (2015b) Use of cyanobacteria and organic fertilizer mixture as soil bioremediation. Am-Eurasian J Agric Environ Sci 15:794–799

Ashrafi A, Zahedi M, Soleimani M (2015) Effect of co-planted purslane (Portulaca oleracea L.) on Cd accumulation by sunflower in different levels of Cd contamination and salinity: a pot study. Int J Phytoremediation 17(9):853–860

Aydinalp C, Marinova S (2009) The effects of heavy metals on seed germination and plant growth on alfalfa plant (Medicago sativa). Bulgarian J Agr Sci 15(4):347–350

Azzarello E, Pandolfi C, Giordano C, Rossi M, Mugnai S, Mancuso S (2012) Ultramorphological and physiological modifications induced by high zinc levels in Paulownia tomentosa. Environ Exp Bot 81:11–17

Bahri B, Zaouchi Y, Laribi B, Rezgui S, Bettaieb T (2014) Photosynthetic performance of Paulownia tomentosa (Thunb.) Steud. exposed to heavy metals zinc and cadmium. Greener J Agric Sci 4:171–177

BaratzadehPoustchi F, Tabatabaei Yazdi F, Heidari A, Moosavi Z (2020) Evaluation of chromium accumulation and resulting histopathological changes in Libyan jirds (Mammals, Rodentia), affected by effluent from Ghazghan leather industrial town, Iran. Environ Sci Pollut Res 27(31):39343–39353

BiglariQuchanAtigh Z, Heidari A, Sepehr A, Bahreini M, Mahbub K (2020) Bioremediation of heavy metal contaminated soils originated from iron ore mine by bio-augmentation with native cyanobacteria. Iran (Iranica) J Energy Environ 11(2):89–96

Bremner J (1960) Determination of nitrogen in soil by the Kjeldahl method. J Agric Sci 55(1):11–33

Buzan RL, Maxim A, Odagiu A, Balint C, Hartagan RM (2018) Paulownia sp. used as an energetic plant, for the phytoremediation of soils and in agroforestry systems. ProEnvironment Promediu 11(34)

Cameselle C, Gouveia S, Urréjola S (2019) Benefits of phytoremediation amended with DC electric field. Application to soils contaminated with heavy metals. Chemosphere 229:481–488

Cao L, Jiang M, Zeng Z, Du A, Tan H, Liu Y (2008) Trichoderma atroviride F6 improves phytoextraction efficiency of mustard (Brassica juncea (L.) Coss. var. foliosa Bailey) in Cd, Ni contaminated soils. Chemosphere 71(9):1769–1773

Chen X, Wu C, Tang J, Hu S (2005) Arbuscular mycorrhizae enhance metal lead uptake and growth of host plants under a sand culture experiment. Chemosphere 60(5):665–671

Citterio S, Prato N, Fumagalli P, Aina R, Massa N, Santagostino A, Sgorbati S, Berta G (2005) The arbuscular mycorrhizal fungus Glomus mosseae induces growth and metal accumulation changes in Cannabis sativa L. Chemosphere 59(1):21–29

Dorjee P, Amarasiriwardena D, Xing B (2014) Antimony adsorption by zero-valent iron nanoparticles (nZVI): ion chromatography–inductively coupled plasma mass spectrometry (IC–ICP-MS) study. Microchem J 116:15–23

Doumett S, Lamperi L, Checchini L, Azzarello E, Mugnai S, Mancuso S, Petruzzelli G, Del Bubba M (2008) Heavy metal distribution between contaminated soil and Paulownia tomentosa, in a pilot-scale assisted phytoremediation study: influence of different complexing agents. Chemosphere 72(10):1481–1490

Doumett S, Fibbi D, Azzarello E, Mancuso S, Mugnai S, Petruzzelli G, Del Bubba M (2010) Influence of the application renewal of glutamate and tartrate on Cd, Cu, Pb and Zn distribution between contaminated soil and Paulownia tomentosa in a pilot-scale assisted phytoremediation study. Int J Phytorem 13(1):1–17

Fajardo C, Ortíz L, Rodríguez-Membibre M, Nande M, Lobo M, Martin M (2012) Assessing the impact of zero-valent iron (ZVI) nanotechnology on soil microbial structure and functionality: a molecular approach. Chemosphere 86(8):802–808

Forte J, Mutiti S (2017) Phytoremediation potential of Helianthus annuus and Hydrangea paniculata in copper and lead-contaminated soil. Water Air Soil Pollut 228(2):77

Gil-Díaz M, Diez-Pascual S, González A, Alonso J, Rodríguez-Valdés E, Gallego J, Lobo MC (2016) A nanoremediation strategy for the recovery of an As-polluted soil. Chemosphere 149:137–145

Gomes HI (2012) Phytoremediation for bioenergy: challenges and opportunities. Environ Technol Rev 1(1):59–66

Gupta RK, Choudhary KK, Kumar M, Negi A, Rai H (2012) Bioremediation and cyanobacteria an overview. BioNano Front 9:190–196

Han Y-H, Liu X, Rathinasabapathi B, Li H-B, Chen Y, Ma LQ (2017) Mechanisms of efficient As solubilization in soils and As accumulation by As-hyperaccumulator Pteris vittata. Environ Pollut 227:569–577

Han Z, Wan D, Tian H, He W, Wang Z, Liu Q (2019) Pollution assessment of heavy metals in soils and plants around a molybdenum mine in central China. Pol J Environ Stud 28(1):123–133

Hansel C, Learman D, Lentini C, Ekstrom E (2011) Effect of adsorbed and substituted Al on Fe (II)-induced mineralization pathways of ferrihydrite. Geochim Cosmochim Acta 75(16):4653–4666

Hidalgo KTS, Carrión-Huertas PJ, Kinch RT, Betancourt LE, Cabrera CR (2020) Phytonanoremediation by Avicennia germinans (black mangrove) and nano zero valent iron for heavy metal uptake from Cienaga Las Cucharillas wetland soils. Environ Nanotechnol Monit Manag 14:100363

Huang D, Qin X, Peng Z, Liu Y, Gong X, Zeng G, Huang C, Cheng M, Xue W, Wang X (2018) Nanoscale zero-valent iron assisted phytoremediation of Pb in sediment: impacts on metal accumulation and antioxidative system of Lolium perenne. Ecotoxicol Environ Saf 153:229–237

Jesitha K, Harikumar PS (2018) Application of nano-phytoremediation technology for soil polluted with pesticide residues and heavy metals. In: Phytoremediation: management of environmental contaminants, vol 6. pp 415–439

Jiang D, Zeng G, Huang D, Chen M, Zhang C, Huang C, Wan J (2018) Remediation of contaminated soils by enhanced nanoscale zero valent iron. Environ Res 163:217–227

Chittora D, Meena M, Barupal T, Swapnil P, Sharma K (2020) Cyanobacteria as a source of biofertilizers for sustainable agriculture. Biochemistry biophysics reports 22:100737

Kheirfam H, Roohi M (2020) Accelerating the formation of biological soil crusts in the newly dried-up lakebeds using the inoculation-based technique. Sci Total Environ 706:136036

Killham KA, Firestone M (1983) Vesicular arbuscular mycorrhizal mediation of grass response to acidic and heavy metal depositions. Plant Soil 72:39–48

Krishnamoorthy R, Venkatramanan V, Senthilkumar M, Anandham R, Kumutha K, Sa T (2019) Management of heavy metal polluted soils: perspective of arbuscular mycorrhizal fungi. Sustain Green Technol Environ Manag 67–85

Leung H-M, Zhen-Wen W, Zhi-Hong Y, Kin-Lam Y, Xiao-Ling P, Cheung K-C (2013) Interactions between arbuscular mycorrhizae and plants in phytoremediation of metal-contaminated soils: a review. Pedosphere 23(5):549–563

Li H, Zhao Q, Huang H (2019) Current states and challenges of salt-affected soil remediation by cyanobacteria. Sci Total Environ 669:258–272

Li Y, Zhao H-P, Zhu L (2021) Remediation of soil contaminated with organic compounds by nanoscale zero-valent iron: a review. Sci Total Environ 760:143413

Liu Y-J, Zhu Y-G, Ding H (2007) Lead and cadmium in leaves of deciduous trees in Beijing, China: development of a metal accumulation index (MAI). Environ Pollut 145(2):387–390

Liu M, Wang J, Xu M, Tang S, Zhou J, Pan W, Ma Q, Wu L (2022) Nano zero-valent iron-induced changes in soil iron species and soil bacterial communities contribute to the fate of Cd. J Hazard Mater 424:127343

Ma X, Gurung A, Deng Y (2013) Phytotoxicity and uptake of nanoscale zero-valent iron (nZVI) by two plant species. Sci Total Environ 443:844–849

Ma Y, Rajkumar M, Oliveira RS, Zhang C, Freitas H (2019) Potential of plant beneficial bacteria and arbuscular mycorrhizal fungi in phytoremediation of metal-contaminated saline soils. J Hazard Mater 379:120813

Mar Gil-Díaz M, Pérez-Sanz A, Angeles Vicente M, Carmen Lobo M (2014) Immobilisation of Pb and Zn in soils using stabilised zero-valent iron nanoparticles: effects on soil properties. Clean-Soil Air Water 42(12):1776–1784

Marrugo-Negrete J, Durango-Hernández J, Pinedo-Hernández J, Olivero-Verbel J, Díez S (2015) Phytoremediation of mercury-contaminated soils by Jatropha curcas. Chemosphere 127:58–63

Mohammadpouran HR, Fotovat A, Haghnia GH, Halajnia A, Chomsaz M (2009) The effect of leather processing industries' waste water on chromium and its fractions in soil. J Water Soil 23(2):10. http://www.magiran.com/p656963

Mokarram-Kashtiban S, Hosseini SM, Kouchaksaraei MT, Younesi H (2019) The impact of nanoparticles zero-valent iron (nZVI) and rhizosphere microorganisms on the phytoremediation ability of white willow and its response. Environ Sci Pollut Res 26(11):10776–10789

Mylavarapu R, Bergeron J, Wilkinson N, Hanlon EA (2020) Soil pH and electrical conductivity: a county extension soil laboratory manual. EDIS 2020(1)

Nisha R, Kiran B, Kaushik A, Kaushik C (2018) Bioremediation of salt affected soils using cyanobacteria in terms of physical structure, nutrient status and microbial activity. Int J Environ Sci Technol 15:571–580

Olsen SR (1954) Estimation of available phosphorus in soils by extraction with sodium bicarbonate. US Department of Agriculture No. 939

Park C-H, Li XR, Zhao Y, Jia RL, Hur J-S (2017) Rapid development of cyanobacterial crust in the field for combating desertification. PLoS One 12(6):e0179903

Parmar S, Singh V (2015) Phytoremediation approaches for heavy metal pollution: a review. J Plant Sci Res 2(2):135

Pavelková A, Cencerová V, Zeman J, Antos V, Nosek J (2021) Reduction of chlorinated hydrocarbons using nano zero-valent iron supported with an electric field. Characterization of electrochemical processes and thermodynamic stability. Chemosphere 265:128764

Phillips J, Hayman D (1970) Improved procedures for clearing roots and staining parasitic and vesicular-arbuscular mycorrhizal fungi for rapid assessment of infection. Trans Br Mycol Soc 55(1):158-IN18

Poveda J (2021) Cyanobacteria in plant health: biological strategy against abiotic and biotic stresses. Crop Prot 141:105450

Ramakrishnan B, Raju MN, Venkateswarlu K, Megharaj M (2023) Potential of microalgae and cyanobacteria in improving soil health and agricultural productivity—a critical view. Environ Sci: Adv

Riaz M, Kamran M, Fang Y, Wang Q, Cao H, Yang G, Deng L, Wang Y, Zhou Y, Anastopoulos I (2021) Arbuscular mycorrhizal fungi-induced mitigation of heavy metal phytotoxicity in metal contaminated soils: a critical review. J Hazard Mater 402:123919

Román JR, Roncero-Ramos B, Chamizo S, Rodríguez-Caballero E, Cantón Y (2018) Restoring soil functions by means of cyanobacteria inoculation: importance of soil conditions and species selection. Land Degrad Dev 29(9):3184–3193

Rowell DL (1994) Soil science: methods and applications. 350 pp. Harlow: Longman Group 郾

Sang L, Wang G, Liu L, Bian H, Jiang L, Wang H, Zhang Y, Zhang W, Peng C, Wang X (2021) Immobilization of Ni (II) at three levels of contaminated soil by rhamnolipids modified nano zero valent iron (RL@ nZVI): effects and mechanisms. Chemosphere 276:130139

Saravanan A, J R, Hemavathy RV, Jeevanantham S, Hamsini S, Senthil Kumar P, Yaashikaa PR, Manivasagan V, Yuvaraj D (2019) Phytoremediation of Cr(VI) ion contaminated soil using Black gram (Vigna mungo): assessment of removal capacity. J Environ Chem Eng 7(3):103052

Sekabira K, Oryem–Origa H, Mutumba G, Kakudidi E, Basamba TA (2011) Heavy metal phytoremediation by Commelina benghalensis (L) and Cynodon dactylon (L) growing in urban stream sediments. Plant Physiol Biochem 3:133–142

Shah V, Daverey A (2020) Phytoremediation: a multidisciplinary approach to clean up heavy metal contaminated soil. Environ Technol Innov 18:100774

Singh V, Singh D (2015) Cyanobacteria modulated changes and its impact on bioremediation of saline-alkaline soils. Bangladesh J Bot 44(4):653–658

Song B, Xu P, Chen M, Tang W, Zeng G, Gong J, Zhang P, Ye S (2019) Using nanomaterials to facilitate the phytoremediation of contaminated soil. Crit Rev Environ Sci Technol 49(9):791–824

Su H, Fang Z, Tsang PE, Zheng L, Cheng W, Fang J, Zhao D (2016) Remediation of hexavalent chromium contaminated soil by biochar-supported zero-valent iron nanoparticles. J Hazard Mater 318:533–540

Tafazoli M, Hojjati SM, Biparva P, Kooch Y, Lamersdorf N (2020) Efficiency of iron nanoparticles and cellulosic wastes for reclamation of lead contaminated soil and oak seedling establishments. J Environ Sci Technol 22(2):43–55

Tian D, Jiang Z, Jiang L, Su M, Feng Z, Zhang L, Wang S, Li Z, Hu S (2019) A new insight into lead (II) tolerance of environmental fungi based on a study of Aspergillus niger and Penicillium oxalicum. Environ Microbiol 21(1):471–479

Ullah R, Hadi F, Ahmad S, Jan AU, Rongliang Q (2019) Phytoremediation of lead and chromium contaminated soil improves with the endogenous phenolics and proline production in Parthenium, Cannabis, Euphorbia, and Rumex species. Water Air Soil Pollut 230:1–13

Vilela LAF, Barbosa MV (2019) Contribution of arbuscular mycorrhizal fungi in promoting cadmium tolerance in plants. In: Cadmium tolerance plants. Academic Press, pp 553–586

Wong CC, Wu SC, Kuek C, Khan AG, Wong MH (2007) The role of mycorrhizae associated with vetiver grown in Pb-/Zn-contaminated soils: greenhouse study. Restor Ecol 15(1):60–67

Wu S, Zhang X, Sun Y, Wu Z, Li T, Hu Y, Su D, Lv J, Li G, Zhang Z (2015) Transformation and immobilization of chromium by arbuscular mycorrhizal fungi as revealed by SEM–EDS, TEM–EDS, and XAFS. Environ Sci Technol 49(24):14036–14047

Wuana R, Okieimen F, Imborvungu J (2010) Removal of heavy metals from a contaminated soil using organic chelating acids. Int J Environ Sci Technol 7:485–496

Xu P, Zeng GM, Huang DL, Feng CL, Hu S, Zhao MH, Lai C, Wei Z, Huang C, Xie GX, Liu ZF (2012a) Use of iron oxide nanomaterials in wastewater treatment: a review. Sci Total Environ 424:1–10

Xu P, Zeng GM, Huang DL, Lai C, Zhao MH, Wei Z, Li NJ, Huang C, Xie GX (2012b) Adsorption of Pb(II) by iron oxide nanoparticles immobilized Phanerochaete chrysosporium: equilibrium, kinetic, thermodynamic and mechanisms analysis. Chem Eng J 203:423–431

Yoon J, Cao X, Zhou Q, Ma LQ (2006) Accumulation of Pb, Cu, and Zn in native plants growing on a contaminated Florida site. Sci Total Environ 368(2–3):456–464

Zhang M, Wang Y, Zhao D, Pan G (2010) Immobilization of arsenic in soils by stabilized nanoscale zero-valent iron, iron sulfide (FeS), and magnetite (Fe 3 O 4) particles. Chin Sci Bull 55(4):365–372

Zhang M, Chen Y, Du L, Wu Y, Liu Z, Han L (2020) The potential of Paulownia fortunei seedlings for the phytoremediation of manganese slag amended with spent mushroom compost. Ecotoxicol Environ Saf 196:110538

Zulfiqar U, Haider FU, Ahmad M, Hussain S, Maqsood MF, Ishfaq M, Shahzad B, Waqas MM, Ali B, Tayyab MN (2023) Chromium toxicity, speciation, and remediation strategies in soil-plant interface: a critical review. Front Plant Sci 13:1081624